The Thesis Committee for Alissa Neuhausen
Certifies that this is the approved version of the following thesis:

Tensile Behavior of Expansion and Undercut Anchors in Concrete Affected by Alkali-Silica Reaction

APPROVED BY
SUPERVISING COMMITTEE:

Oguzhan Bayrak, Supervisor

David J. Eaton, Co-Supervisor

Richard E. Klingner

Tensile Behavior of Expansion and Undercut Anchors in Concrete Affected by Alkali-Silica Reaction

by

Alissa Neuhausen, B.S.

Thesis

Presented to the Faculty of the Graduate School of

The University of Texas at Austin

in Partial Fulfillment

of the Requirements

for the Degree of

Master of Science in Engineering

Master of Public Affairs

The University of Texas at Austin

August 2014

Dedication

In memory of my parents who gave me confidence and inspired me to never give up.

This work is dedicated to them.

Acknowledgements

This thesis would not have been possible without the help of many people.

I am especially grateful to my advisor Dr. Klingner. I would have neither started the project nor finished my thesis without your support and encouragement.

This project would not have been possible without the sponsorship of MPR Associates Your presence at the lab was always noticed.

I would also like to thank my fellow graduate researchers, who not only made working enjoyable, but whose friendship was invaluable. They include Anthony DeFurio, Josh Ramirez, and Patrick Short. Thanks to Nick Dassow and Trey Dondrea for helping wrap up the anchor testing. Thanks to Gloriana Arrieta, David Wald, Beth Zetzman, Joseph Klein, Sara Watts, and Daniel Elizondo for our lively lunchtime conversations that made the days feel shorter.

I would also like to thank the FSEL staff: Dennis Fillip, Blake Stasney, David Braley, and Eric Schell for always providing assistance on the lab floor and sharing your expertise. Thanks to Barbara Howard and Michelle Damvar for all of the administrative assistance.

Finally, thanks to NSF for their financial support of my education. This material is based upon work supported by the National Science Foundation Graduate Research Fellowship under Grant No. DGE-1110007. Any opinion, findings, and conclusions or recommendations expressed in this material are those of the author and do not necessarily reflect the views of the National Science Foundation.

Abstract

Tensile Behavior of Expansion and Undercut Anchors in Concrete Affected by Alkali-Silica Reaction

Alissa Neuhausen, M.S.E., M.P.Aff.

The University of Texas at Austin, 2014

Supervisors: Oguzhan Bayrak, David J. Eaton

This thesis addresses the tensile capacity and load-deflection behavior of wedge-type expansion and undercut anchors in concrete affected by alkali-silica reaction (ASR). ASR is a chemical reaction that occurs between alkalis in the cement and silica in the aggregates. The reaction occurs with the presence of moisture, forming a gel which expands and causes micro-cracking in the concrete. Researchers conducted 85 static unconfined tensile tests on control and ASR-affected specimens. The results indicate that anchors in concrete cracked due to ASR perform like anchors in concrete cracked due to other mechanisms. Up to a threshold value of the Comprehensive Crack Index (CCI) of at least 1.5 mm/m, all cracking, regardless of cause, has the same effect on the tensile breakout capacity of mechanical and undercut anchors.

Table of Contents

List of Tables

List of Figures

CHAPTER 1
Introduction

1.1 OVERVIEW

Over their lifetimes, concrete structures undergo changing stress conditions as a result of the environmental conditions to which they are exposed. One such stress condition is alkali-silica reaction (ASR) a consequence of the exposure of certain concrete mixtures to a combination of high temperatures and humidity. ASR alters the engineering properties of concrete over time, presenting challenges for assessing existing structures without extensive destructive testing. This report examines the effects of ASR on the behavior of post-installed expansion and undercut anchors.

Anchors transfer load from an attachment into a concrete structural element, and are often used to connect structural elements or mechanical equipment to concrete floors, walls, or ceilings. Anchor performance is critical to the behavior of these attachments, many of which may be components that are safety-related or otherwise important to the functionality of the structure.

To ensure proper behavior of such attachments, it is important to understand how the presence of ASR affects the performance of anchors. Although anchor behavior in cracked and uncracked concrete has been extensively researched and codified, this research has not considered behavior in cracks due to ASR. The research project detailed in this report covers the investigation of the influence of ASR on the tensile capacity and load-displacement behavior of mechanical wedge-type expansion anchors and undercut anchors at a variety of embedment depths. The conclusions drawn are based on predictions using current design equations from ACI 318-11 for anchors embedded in cracked concrete.

The problem of ASR deterioration in concrete has been recognized for over half a century. Structures in over 100 countries have been diagnosed with ASR deterioration. This has led to research on the effect of ASR in numerous countries including Canada,

Korea, Germany, and the United States. The challenge in ASR research is to be able to apply results generically over a wider range of mixtures and elements. Because the progression of ASR depends on many factors, including alkali content, aggregate reactivity, and environmental conditions, results from previous research cannot yet be used to predict the behavior in general of structures undergoing ASR deterioration. Because ASR deterioration varies from structure to structure, large-scale testing is necessary to replicate actual conditions. Such research must be transferable from the laboratory to the field, particular when it is used to evaluate existing structures.

1.2 OBJECTIVES AND SCOPE OF THESIS

This research project occurred in two phases. The first phase took place from December 2011 to February 2012. The second phase began immediately following the first, and is still ongoing. This thesis covers the second phase only. The project was sponsored and overseen by MPR Associates (Arlington, VA). The work was carried out by the Ferguson Structural Engineering Laboratory (FSEL) of The University of Texas at Austin. To ensure traceable conformance with industry standards, the work was conducted under a strict quality assurance program, including testing protocols, equipment calibration, personnel training, and data archiving.

The first phase included testing of anchors in existing bridge girders, stored at Ferguson Laboratory, which exhibited ASR deterioration and delayed ettringite formation (DEF). Confined (pullout) tests and unconfined (breakout) tension tests were performed on wedge-type expansion and undercut anchors installed in these girders. Those tests involved a single anchor diameter and a single embedment depth. The second phase was established to address the fact that the girders of Phase 1 had not been controlled by FSEL over their lifetime. The second phase included new specimens cast at FSEL, using high-alkali mixture designs, high-temperature curing, and exposure to controlled cycles of wetting and drying, all of which had been shown in previous FSEL projects to develop the rapid progression of ASR. Starting from the time of casting and throughout the life of the specimens, their ASR levels were tracked using indices of surface cracking. Some

anchors were installed in control specimens (no ASR damage); other anchors were installed in ASR-prone specimens, which were then monitored as ASR developed ("pre-ASR specimens"); and still other anchors were installed in specimens with existing ASR damage ("post-ASR specimens").

The installed anchors were tested to failure in tension in an unconfined condition, permitting tensile breakout. For different levels of controlled ASR damage, the performance of anchors installed in the pre-ASR specimens and the post-ASR specimens was compared with that of anchors installed in the control specimens. These results were used to establish a correlation between ASR deterioration and anchor capacity, and between ASR deterioration and anchor capacity as predicted by current design equations.

1.3 ORGANIZATION OF THESIS

This thesis is organized into six chapters: background information (Chapter 2), development of the testing program (Chapter 3), test results (Chapter 4), a discussion of the results (Chapter 5), and conclusions and recommendations (Chapter 6).

The information provided in *Chapter 2* outlines relevant background information on the tensile testing of anchors (Section 2.1 – 2.6). Prior tensile testing of anchors examined both anchor capacity and load-deflection behavior. That research includes testing in both cracked and uncracked concrete for all types of anchors. Much of that research was used to develop the Concrete Capacity Design Method and to establish the technical basis for ACI 318 Appendix D. That chapter also contains relevant information on the laboratory methods used to promote the accelerated growth of ASR, the detection and measurement of ASR, and the engineering properties of ASR-affected concrete (Section 2.7 – 2.8).

The testing program explained in *Chapter 3* provides detailed information on the work performed by researchers at FSEL. The chapter includes information on casting the concrete specimens (Section 3.2) using knowledge from prior research projects conducted at FSEL on beams with ASR deterioration. Also included is information related to the installation of torque-controlled, wedge-type expansion anchors and

undercut anchors (Section 3.5). The final section (Section 3.6) details the tensile test setup, instrumentation, and data collection.

The results of the experimental program are presented in *Chapter 4*, and discussed in *Chapter 5*. The results include the quantification of ASR deterioration for each of the tested specimens, the normalized tensile capacity of anchors with respect to ASR levels and embedment depths, and typical load-displacement curves for each anchor type. The discussion includes statistical characteristics of the experimentally determined capacities for each anchor type. The concluding chapter, *Chapter 6*, includes code implications and recommendations for future testing of concrete anchors embedded in ASR-affected concrete.

CHAPTER 2
Background

2.1 OVERVIEW

The purpose of this chapter is to summarize current knowledge related to the behavior of post-installed mechanical anchors and to alkali-silica reaction (ASR). These topics are fundamental to the testing program detailed in Chapter 3, which consists of unconfined static tensile testing on wedge-type expansion and undercut anchors installed in ASR-affected concrete. The results provide insight into the behavior of anchors in concrete cracked as a result of ASR compared to concrete cracked due to other mechanisms. Some of the information in Chapter 2 is also used in Chapter 5 to assess the consistency of the results generated under this testing program.

The first topic in Chapter 2 is the behavior of anchors in uncracked concrete (Sections 2.2 – 2.5). The behavior is primarily explained from the perspective of design documents (ACI 318 and ACI 349), with emphasis on wedge-type expansion and undercut anchors. Potential failure modes for each anchor type are described, along with a brief explanation of the difference between confined and unconfined tensile tests. The next section incorporates the effects of cracked concrete into the discussion of anchor behavior (Sections 2.6), and includes a description of the expected changes in anchor capacity and load-displacement behavior as a result of cracking. The final section of the chapter includes an explanation of ASR, of the laboratory methods for accelerating the growth of ASR in concretes intentionally produced to show ASR (Section 2.7), and of the anticipated effects of ASR on anchor performance (Section 2.8).

2.2 TYPES OF ANCHORS

Anchors are used to transfer loads from steel or other attachments into concrete members. Some anchor types along with their respective resistance mechanisms are depicted in Figure 2-1. The anchor types important to this thesis have bold borders.

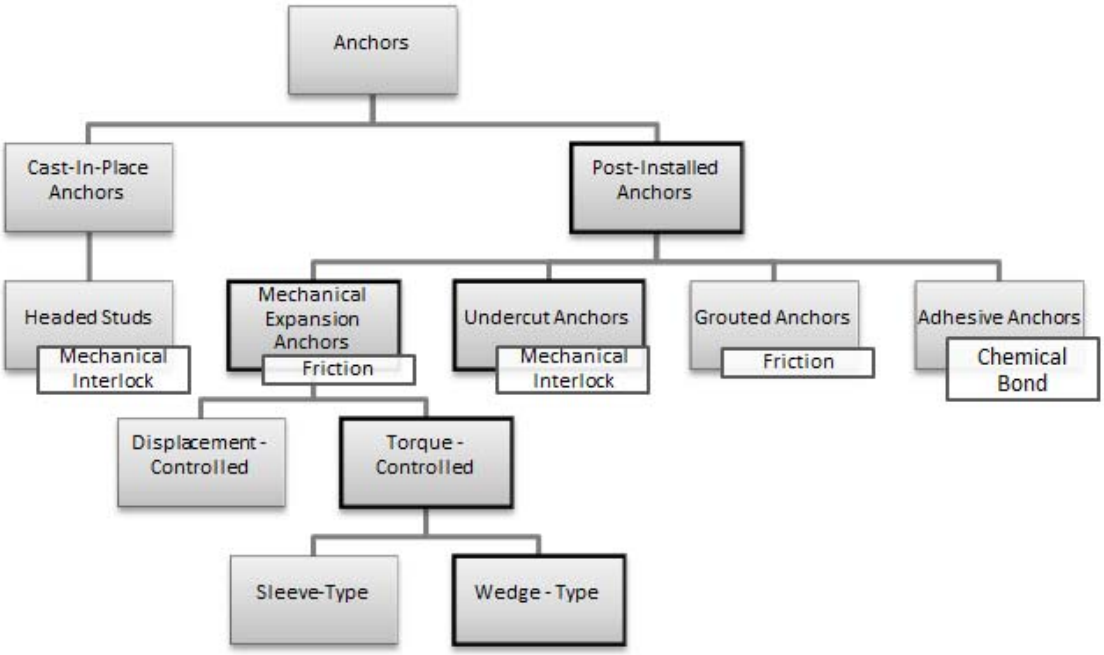

Figure 2-1: Types of Anchors and Load Transfer Mechanisms

Cast-in-place anchors are installed prior to concrete placement, and include headed studs and headed bolts. Post-installed anchors are installed in hardened concrete, and include mechanical anchors and bonded anchors. Post-installed mechanical anchors can be broadly categorized as expansion anchors and undercut anchors.

2.3 BEHAVIOR OF POST –INSTALLED ANCHORS

The post-installed anchors important to this thesis are wedge-type expansion anchors and undercut anchors. Each is described in more detail below.

2.3.1 Expansion Anchors

As shown in Figure 2-2, mechanical expansion anchors transfer force through friction between the expansion element (clip or sleeve) and the surrounding concrete.

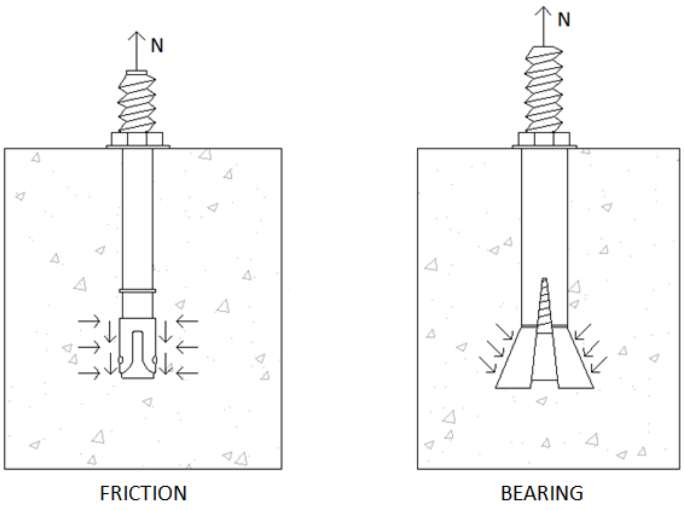

Figure 2-2: Force-transfer Mechanisms for Expansion Anchors (friction) and Undercut Anchors (bearing)

Friction is created by forcing the conical wedge against the expansion element causing the expansion element to spread. Because the drilled hole for an expansion anchor is equal to the anchor diameter, the expansion element spreads into the surrounding concrete. Figure 2-3 shows the main components of an expansion anchor.

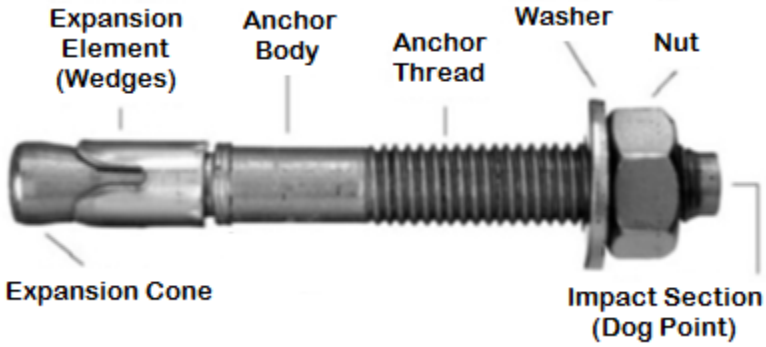

Figure 2-3: Components of Typical Torque-controlled Expansion Anchor (Hilti. 2011)

For torque-controlled anchors, torque applied to the anchor nut draws the conical wedge into the expansion element. Applied load causes the expansion element to expand further, possibly increasing friction with the surrounding concrete. For displacement-controlled expansion anchors, driving an expansion plug into the expansion element

forces it to expand against the concrete. Because additional applied tension does not improve the behavior of the resistance mechanism (Eligehausen 2006), displacement-controlled expansion anchors are not approved by ACI 318 or ACI 349 for use in cracked concrete.

Expansion anchors loaded in tension can fail by the entire anchor pulling out of the drilled hole (pull-out failure) or by the anchor pulling through the expansion element (pull-through failure). At smaller embedment depths, expansion anchors can also exhibit concrete breakout failure. ACI 318 requires qualification consistent with ACI 355.2 for design against pull-out and pull-through failures, and provides design equations for concrete breakout failure of expansion anchors.

2.3.2 Undercut Anchors

As shown in Figure 2-1, undercut anchors transfer force through bearing of the anchor against the undercut portion of the drilled hole. The undercut is made by locally widening an area near the base of the drilled hole. Torqueing the anchor opens the anchor against the undercut, so that the anchor then bears against the inclined sides of the undercut. A typical undercut anchor is shown in Figure 2-4.

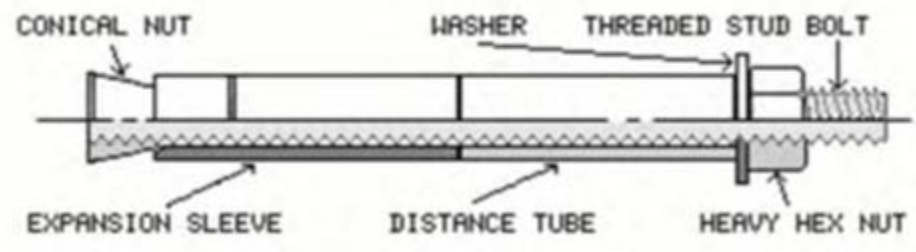

Figure 2-4: Example Undercut and Anchor and Component Parts (ICBO. 1992)

Undercut anchors are designed to fail by steel yield or concrete breakout. In predicting breakout capacities, undercut anchors are treated as cast-in-place anchors. Undercut anchors behave more like headed studs than other post-installed anchors (Pusill-Wachtsmuth 2001).

2.3.3 Building Code Treatment of Post-Installed Anchors

In the US, the design of anchors is governed by state and model codes, which reference ACI 318. Requirements for the tensile and shear capacity of cast-in anchors, expansion anchors, and undercut anchors are included in Appendix D of ACI 318. Qualification is not needed for cast-in-place headed anchors. Qualification of post-installed anchors is addressed by ACI 355.2 *Qualification of Post-Installed Mechanical Anchors in* Concrete and ACI 355.4 *Qualification for Post-Installed Adhesive Anchors in Concrete.*

Design requirements for anchorage to concrete for nuclear structures are provided in ACI 349 *Code Requirements for Nuclear Safety-Related Structures*. Historically, ACI 349 differed from ACI 318 in the treatment of concrete cone breakout failures and the seismic design of anchors; however, ACI 349-06 has adopted many of the provisions incorporated into ACI 318-02 and later versions (Mahrenholtz and Eligehausen 2013). Another significant change in ACI 349 was to relax the requirement that anchor behavior be governed by steel failure for nuclear applications (Rodriguez 1995). This permitted more harmonization between those two design documents.

2.4 FAILURE MODES OF ANCHORS SUBJECTED TO TENSILE LOADING

The important failure modes for single anchors in tension away from edges are concrete cone breakout, steel fracture, pull-out, pull-through, concrete side-face blowout, and splitting. Only the first three are important for the expansion and undercut anchors tested under the anchor program. Of these failure modes, only concrete breakout and pull-out failures are influenced by concrete properties.

2.4.1 Concrete Cone Breakout Failure

Unconfined (breakout) tests determine the concrete cone breakout capacity for anchors in tension. The 1996 database of single anchors in tension included more than 800 tests (Farrow et al. 1996), and has been extensively updated since then. That database was used to validate the Concrete Capacity Design (CCD) Method, an empirical

procedure for predicting the breakout capacity of anchors in ACI 318 and ACI 349. In the CCD equation for breakout capacity (Equation 2-1), f_c' is the specified 28-day concrete compressive strength in psi, h_{ef} is the effective embedment depth in inches, and k_c is a coefficient corresponding to the lower 5% fractile of anchor test results.

$$N_b = k_c\sqrt{f_c'}h_{ef}^{1.5} \qquad \text{Equation 2-1}$$

(Equation D-6 of ACI318-11)

Headed studs and undercut anchors fail in concrete cone breakout below a critical embedment depth (Fuchs et al. 1995). The critical embedment depth, depicted in Figure 2-5, marks the depth at which the governing failure mode switches from concrete breakout to pullout (expansion anchors), or from concrete breakout to steel yield (undercut anchors).

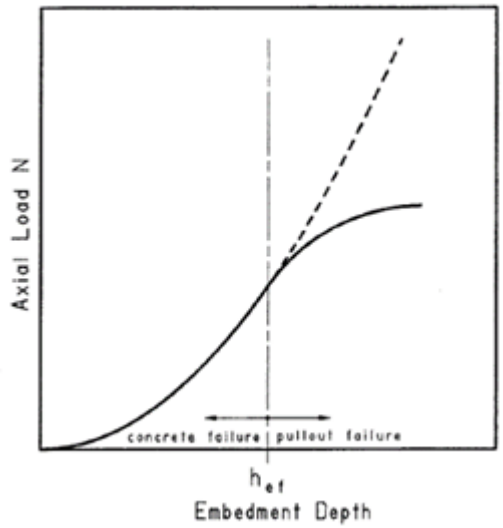

Figure 2-5: Critical Embedment Depth for Expansion Anchors (Fuchs et al. 1995)

2.4.1.1 Effect of Reinforcement on Concrete Breakout Capacity

Reinforcement placed parallel to a concrete surface has a negligible effect on the tensile breakout capacity of anchors oriented perpendicular to the surface. It may even have a negative effect on the concrete cone failure load if the reinforcement bond stresses overlap with anchorage tensile stresses or if the concrete available to transfer tensile

forces is reduced. In contrast, reinforcement placed parallel to the anchor and adequately developed into both the breakout body and the surrounding concrete can increase tensile breakout capacity (Eligehausen et al. 1996; Eligehausen et al. 1989, Hallowell 1996).

2.4.2 Steel Failure

As shown by Equation 2-2 below, tensile capacity as governed by steel fracture depends on $A_{se,N}$ (the effective cross-sectional area of the anchor in tension and f_{uta}(the specified tensile strength of the anchor steel). Failure as governed by steel yield and fracture has a lower coefficient of variation than failure as governed by concrete breakout (Nowak and Collins 2013).

$$N_{sa} = A_{se,N} f_{uta}$$ Equation 2-2

(Equation D-2 of ACI318-11)

2.4.3 Pull-out and Pull-through Failure

In pull-out failure, the entire anchor pulls out of the hole, with the expansion element intact. In pull-through failure, the anchor pulls out of the hole, leaving the expansion element behind (Figure 2-6). Because for post-installed anchors this type of failure is anchor-dependent, ACI 318 provides a design equation for the pull-out failure of cast-in headed studs, but requires qualification by ACI 355.2 for post-installed anchors.

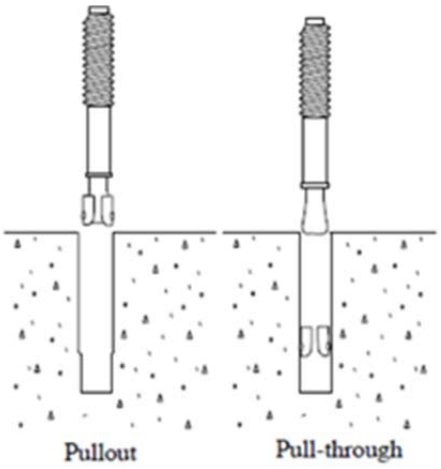

Figure 2-6: Difference between Pull-out and Pull-Through Failures (Shirvani 1998)

2.5 TYPES OF TESTING FOR TENSILE ANCHORS

Tensile testing of anchors is intended to determine tensile capacity and load-displacement behavior. Test setups can be confined or unconfined.

2.5.1 Confined Tests of Tensile Anchors

Confined tests, also called pull-out tests, load the anchor in tension with a hydraulic ram that bears directly on the concrete surface, confining the concrete and preventing a concrete breakout failure (Figure 2-7). This type of test was performed at the University of Texas at Austin in 2011 during the first phase of the anchor testing program.

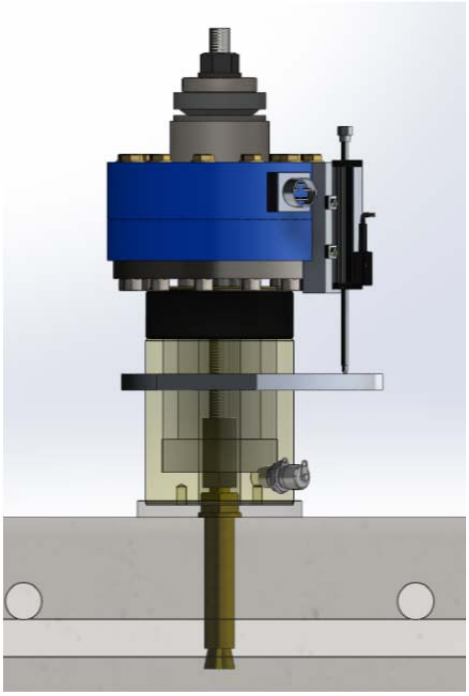

Figure 2-7: Representative Confined Test Setup

2.5.2 Unconfined Tests

Unconfined tests, also known as breakout tests, load the anchor in tension using a reaction device (ring or tripod) that bears against the concrete outside of the projected area of the idealized breakout body (Figure 2-8, Figure 2-9).

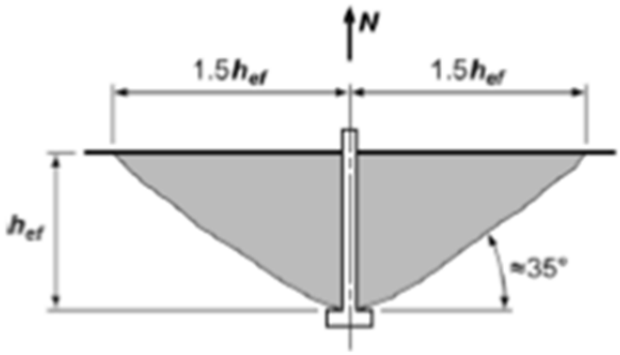

Figure 2-8: Idealized Concrete Cone Breakout Body (ACI 318-11)

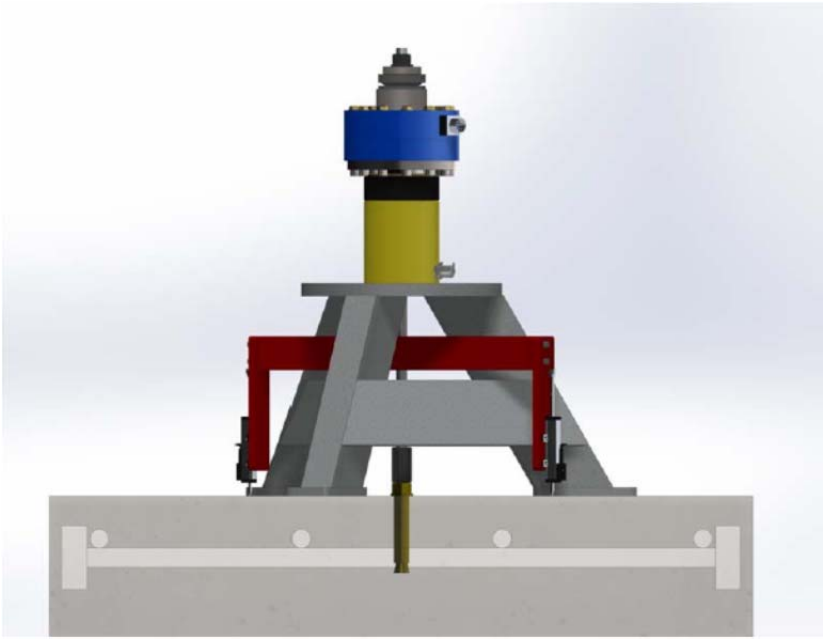

Figure 2-9: Representative Unconfined Test Setup

2.6 EFFECTS OF CRACKED CONCRETE ON ANCHOR BEHAVIOR AND DESIGN

Anchors in concrete are often associated with cracks due to a variety of causes, including installation of a post-installed anchor or the application of load to an anchor. In this section, the effects of that cracking on the fundamental behavior of anchors are reviewed, and the corresponding changes in design equations are summarized.

2.6.1 Effects of Cracking on Concrete Breakout and Pullout Behavior

As shown in Figure 2-10, cracking in concrete near an anchor affects concrete breakout behavior by disrupting the equal distribution of forces in the concrete. In uncracked concrete, local bearing forces around the anchor head are transferred to diagonal compressive struts radiating from the anchor head to the free surface of the concrete in the direction of the applied load. Compression in those struts is equilibrated by circumferential tensile forces in a ring on the free surface.

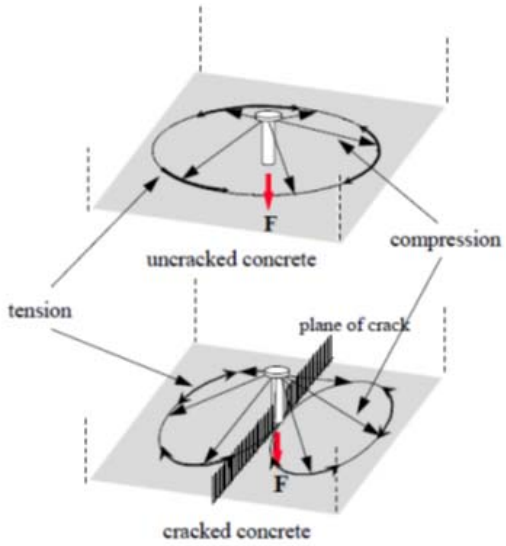

Figure 2-10: Effect of cracking on load-transfer mechanism of headed anchors in tension (Eligehausen and Fuchs 1987)

In cracked concrete, because circumferential tensile stresses cannot be transferred across cracks, the tension ring is replaced by smaller rings and less efficient struts (Eligehausen and Ozbolt 1992). This reduces the anchor's tensile breakout capacity and decreases its stiffness (Figure 2-11).

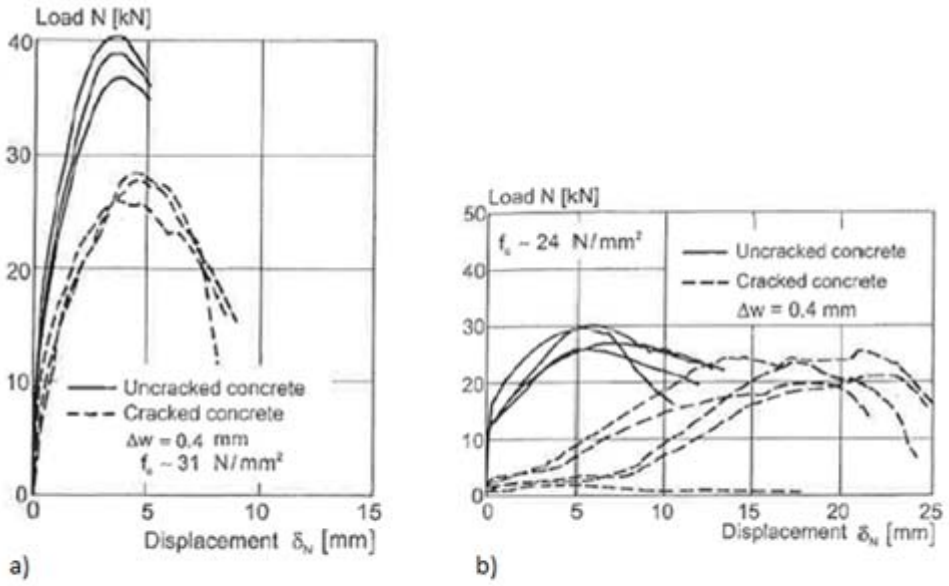

Figure 2-11: Typical Load Displacement Behavior for Torque-Controlled Expansion Anchors in Cracked and Non-Cracked Concrete (Eligehausen et al. 2006)

This decrease in breakout capacity is shown in Figure 2-12(a) and (b) for undercut anchors/headed studs and torque-controlled expansion anchors, respectively. As crack width increases to 0.3-0.4 mm, tensile breakout capacity decreases to 66-75% of the capacity in uncracked concrete. Most of the reduction in capacity occurs for crack widths up to 0.15 mm and flattens out for larger crack widths (Eligehausen and Balogh 1995).

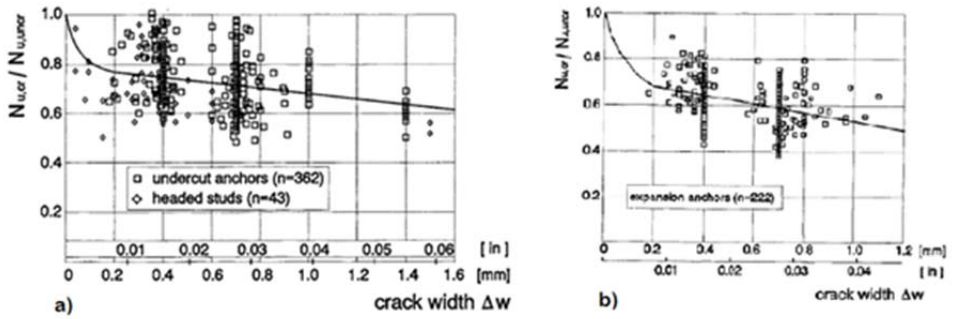

Figure 2-12: Tensile breakout capacities of a)undercut and threaded studs and b) torque-controlled expansion anchors in cracked reinforced concrete as a function of crack width (Eligehausen and Balogh 1995)

A decrease in pull-out capacity is also observed in cracked concrete. The widening of cracks leads to a reduced expansion force and significant displacement beyond low load levels. This leads expansion anchors to expand further, increasing the likelihood of breakout failure in cracked concrete. In contrast, this follow-up expansion would probably have increased the likelihood of pull-out failure in uncracked concrete (Eligehausen and Balogh 1995).

In Appendix D of ACI 318-11, this reduction in tensile breakout capacity as a result of concrete cracking is addressed by the use of a modification factor in the design equations for breakout and pullout failures. Concrete is assumed to be cracked unless demonstrated to be uncracked, giving a modification factor of 1.0 for cracked concrete and 1.4 for uncracked concrete. This corresponds to a capacity in cracked concrete that is 71% of the corresponding capacity in uncracked concrete.

2.6.2 Statistical Variation of Concrete Breakout Capacities in Cracked and Uncracked Concrete

For testing purposes, cracks can be induced in concrete using crack formers (thin metal plates placed before casting the concrete), splitting wedges, a hydraulic expander, or centric tensile loading on reinforcing bars oriented perpendicular to the intended crack direction. For the anchor qualification tests of ACI 355.2, anchors are installed through

hairline cracks, which are then opened to widths of 0.3 mm and 0.5 mm (Eligehausen et al. 2004).

In general, the tensile breakout capacities of anchors installed in cracked and uncracked concrete have similar statistical variations, regardless of how the cracking is induced. The coefficient of variation for undercut anchors and headed studs in cracked concrete is 15.5 percent, no larger than for tests in uncracked concrete. The coefficient of variation for torque-controlled expansion anchors in cracked concrete is 15.8 percent, likewise no larger than for uncracked concrete (Eligehausen and Balogh 1995). This suggests that the behavior of anchors in concrete with cracks of that width, regardless of the cause of those cracks, can be adequately addressed by existing design equations.

2.7 (ASR) ALKALI SILICA REACTION

Alkali-silica reaction (ASR) is a chemical reaction that occurs between alkalis in the cement and silica in the aggregates. The reaction occurs with the presence of moisture, forming a gel which expands and causes micro-cracking in the concrete. The growth rate and ultimate extent of ASR deterioration are affected by the reactivity of the aggregate, relative humidity, temperature, and aggregate particle size. Under field conditions, these factors are generally quite variable, making the growth rate and ultimate extent of ASR deterioration difficult to predict.

2.7.1 Laboratory Techniques for Accelerating ASR Deterioration in Concrete

To investigate the effects of ASR deterioration under laboratory conditions, it is necessary to develop reliable techniques for producing ASR-susceptible concrete and accelerating the development of ASR in that concrete. Such laboratory techniques have been shown to give results comparable to those from in-situ structures (Leemann and Merz 2013).

2.7.2 Concrete Mixture Design and Specimen Conditioning

To produce ASR-affected concrete, it is necessary to use appropriate concrete mixture designs, and to condition specimens appropriately.

2.7.2.1 Portland Cement

Mixture designs for ASR-susceptible concrete can use either Type I or Type III high-alkali cement. Although Type I cement does not accelerate ASR deterioration, it is most common in the field. In contrast, Type III high-alkali cement, while not as common in the field, produces more rapid and more severe ASR deterioration.

2.7.2.2 Fine and Coarse Aggregates

In Texas, Jobe-Newmann sand from El Paso, a fine aggregate with known high silica content and reactivity, has been used in previous projects on ASR at UT Austin. (Folliard et al. 2006). Known reactive coarse aggregates are also available from vendors in many states.

2.7.2.3 Additional Control of Alkalinity

In order for ASR to develop, the alkali content of the concrete mixture consisting of cement, aggregates, admixtures, and any other additions must reach a pH level at least 12.5. To raise the pH of the mixture to this level, laboratories increase the alkali content of the mixture. Past research programs at The University of Texas at Austin have added a sodium hydroxide (NaOH) solution to the mixture (Deschenes 2009).

2.7.2.4 Conditioning

Once specimens have been cast using ASR-susceptible concrete mixtures, accelerating ASR deterioration requires that the specimens be conditioned under high temperatures, high ambient humidity, and wet conditions. Specimens can be kept moist at all times, kept under water at constant temperature, or cycled between wet and dry conditions. Some researchers point to differences between the visible effects of ASR on

specimens cured under water and those which have undergone wet/dry cycles, but one is not conclusively preferred (Folliard et al. 2006; Fournier et al. 2009).

2.7.2.5 BRE Standard Mixture

To compare results among independent projects, the Building Research Establishment (BRE) established a standard mixture for all ASR projects funded by the Science and Engineering Research Council (SERC). This mixture has been used for many European projects testing the engineering properties of ASR-affected concrete (Rigden et al. 1995). For this mixture, both potassium hydroxide (KOH) and NaOH are added to the mixture to increase alkalinity (Rigden et al. 1995). KOH is more typical of aggregates in certain parts of the world, making this addition more representative of typical construction for those regions.

2.7.3 Quantification of ASR Deterioration

How to quantify ASR deterioration has been the subject of much research. Destructive evaluation methods such as the damage rating index (DRI) or materials testing are widely used in laboratory environments, and are discussed briefly here. Non-destructive evaluation methods such the comprehensive crack index (CCI) are more useful for existing structures, however, and are emphasized in the research described here.

2.7.3.1 Destructive Evaluation Methods

Destructive evaluation methods damage the structure, usually through the removal of concrete cores.

2.7.3.1.1 Petrography – Damage Rating Index (DRI)

A petrographic examination entails slicing a concrete core into thin sections for inspection under a microscope. Figure 2-14 illustrates typical petrographic features used to determine the DRI. The letters shown on the above image correspond to the following features: “(a) reaction gel within reacted aggregate; (b) crack in coarse aggregate that

extends into cement paste; (c) crack in cement paste filled with reaction gel; and (d) dark reaction rim surrounding aggregate particle" (Rivard and Ballivy 2005).

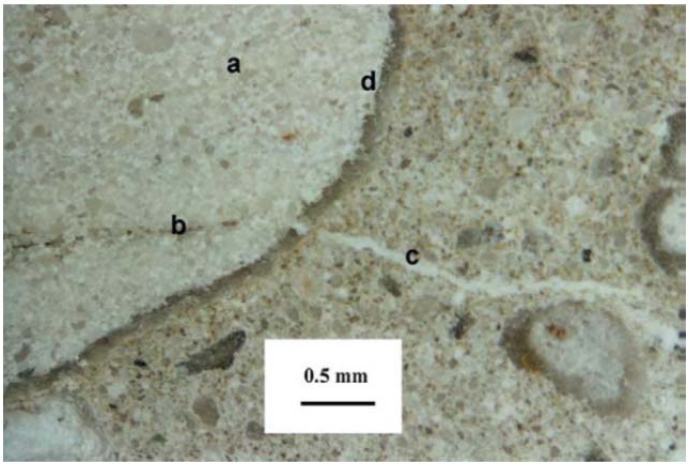

Figure 2-13: Petrographic View of ASR (Rivard, P., Ballivy, G. 2005)

2.7.3.1.2 Materials Testing

Compressive strength, tensile, and modulus testing are materials tests commonly used to diagnose ASR. Previous research has found that although compressive strength is not a good indicator of ASR, tensile strength and modulus are sensitive to the presence of ASR. These methods are good for diagnosing ASR, but not for quantifying its extent across multiple mixtures (Ahmed et al. 2003; Swamy et al. 1988; Giaccio et al. 2008; Smaoui et al. 2006).

2.7.3.2 Non-Destructive Evaluation Methods

Non-destructive evaluation (NDE) methods do not disturb the structural integrity of the concrete on which they are used.

2.7.3.2.1 Comprehensive Crack Index (CCI)

The CCI is the only method used for the research described here, and for that reason is described in detail here. Measurements are recorded as shown on Figure 2-14.

The CCI is determined by measuring crack widths on the surface of the concrete using a crack gauge, loupe, or microscope. The crack widths are measured along lines marked parallel to the directions of surface reinforcement. To calculate the CCI, the summation of the crack widths is then divided by the length of the measuring lines. The CCI is representative of the extent of cracking in the concrete member (Fournier et al. 2010). It can be used to estimate expansion. As the member expands, the difference between the expansion of the confined concrete and the unrestrained cover concrete causes cracking to display on the concrete surface (McLeish 1990).

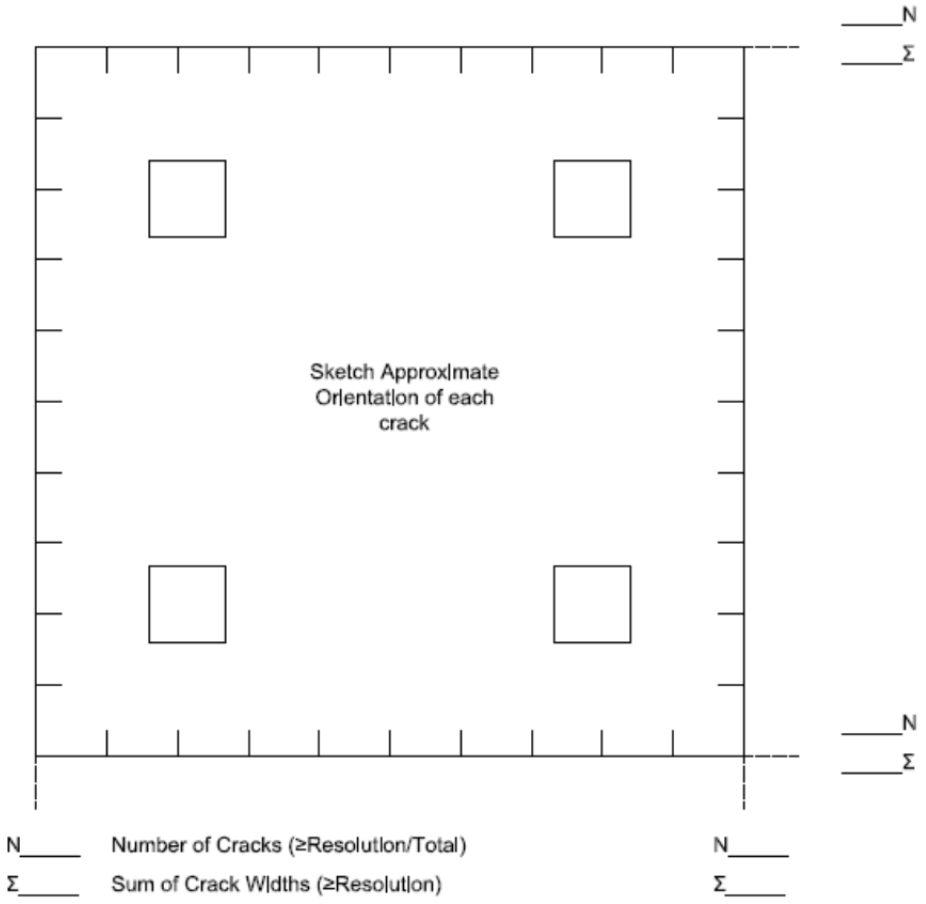

Figure 2-14: Template for Measuring the CCI

The advantages of the CCI are its transparency and simplicity. Its disadvantages are a result of user subjectivity and the variation of crack density along the measuring lines. It is unclear if the CCI can be converted reliably to an expansion measurement,

which would make it more useful for quantifying expansion than for monitoring ASR. The CCI is also sensitive to day-to-day variability in ambient conditions. For the best results, measurements should be taken only during cloudy weather, similar temperatures, and similar humidity conditions (Fournier et al. 2010).

2.7.3.2.2 Expansion Monitoring

Expansion monitoring can be performed on prisms or by installing expansion rods at fixed locations in a structural member. Prisms undergo free expansion, while members undergo confined expansion. Previous research has determined maximum expansion potential as a function of restraint (Jones and Clark 1996). It is generally accepted that confinement does reduce the expansion caused by ASR (Ostertag et al. 2007).

2.8 POTENTIAL EFFECTS OF ALKALI-SILICA REACTION ON ANCHOR CAPACITY

Anchor capacity is lower in cracked concrete than uncracked concrete. The objective of inducing ASR in concrete specimens and testing anchors is to determine whether a difference exists between anchor behavior in concrete cracked due to ASR and in concrete cracked due to other causes.

CHAPTER 3
Development of Testing Program

3.1 OVERVIEW

The testing program described here was developed to intentionally create specimens with extensive ASR deterioration, to examine the behavior of expansion and undercut anchors in those specimens, and to compare that behavior with behavior in control specimens without ASR damage.

This chapter contains an explanation of the second phase of the anchor testing program, conducted between 2011 and 2014. Figure 3-1 shows in schematic form the anchor testing program steps for each specimen. The first third of the chapter includes a description of the methodology used to intentionally produce ASR-affected concrete specimens. It begins with an overview of the concrete specimen design (Section 3.2), continues with an explanation of specimen conditioning (Section 3.3), and ends with an explanation of the ASR monitoring program (Section 3.4). The next part of the chapter (Section 3.5) describes the anchors selected for the program: Torque-Controlled, Wedge-Type Expansion Anchors and Undercut Anchors. The final sections provide information on the test setup, test protocol, instrumentation, and data acquisition (Section 3.6).

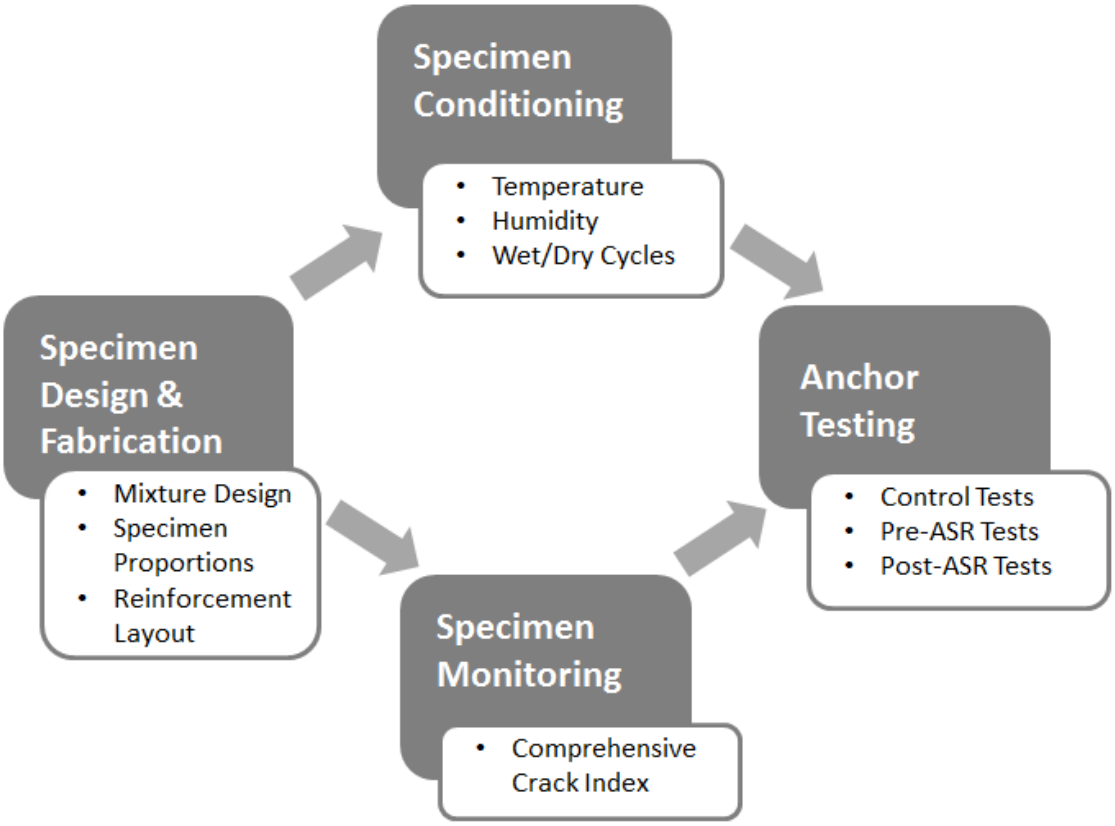

Figure 3-1: –Sequential Organization of Testing Program

3.2 CONCRETE SPECIMENS

The testing program included the fabrication of seven specimens. To date, anchors have been tested in four of the seven specimens. These specimens and their corresponding test descriptions are shown in Table 3-1. The specimens were designed and detailed to perform anchor tests at increasingly severe levels of ASR deterioration determined by CCI measurements.

Table 3-1: Test Specimens

Specimen Designation	Test Type	Testing Completed
AN-01	Post-ASR Installed	Yes
AN-02	Post-ASR Installed	Yes
AN-03	Post-ASR Installed	No
AN-04	Pre-ASR Installed	No
AN-05	Pre-ASR Installed	Yes
AN-06	Pre-ASR Installed	No
AN-07	Control	Yes

3.2.1 Mixture Design

The mixture design for ASR-affected concrete was based on previous successful production of ASR-affected concrete at The University of Texas at Austin over the past decade. It involved high-alkali cement, NaOH-enriched head water, and highly reactive fine aggregate, and is described further in Section 3.2.3.

3.2.2 Specimen Design and Fabrication

As shown in Figure 3-2, specimens were reinforced concrete beams, rectangular in cross-section, with a ratio of height to width of 2.0. Specimens had regularly spaced vertical and horizontal reinforcement on each vertical face. Longitudinal (horizontal) reinforcement consisted of hooked bars, and vertical reinforcement of headed bars (to meet development length requirements). Because the specimens were intended to represent sections of a reinforced concrete wall, they had no reinforcement connecting the grids on each side. To meet proper cover requirements, this required the reinforcing cage to be held in place by form brackets. These had the added benefit of securing and stabilizing the reinforcement cage better than standard ties, allowing less movement of reinforcing bars during specimen fabrication. Figure 3-3 shows the reinforcing cage inside the formwork prior to concrete placement.

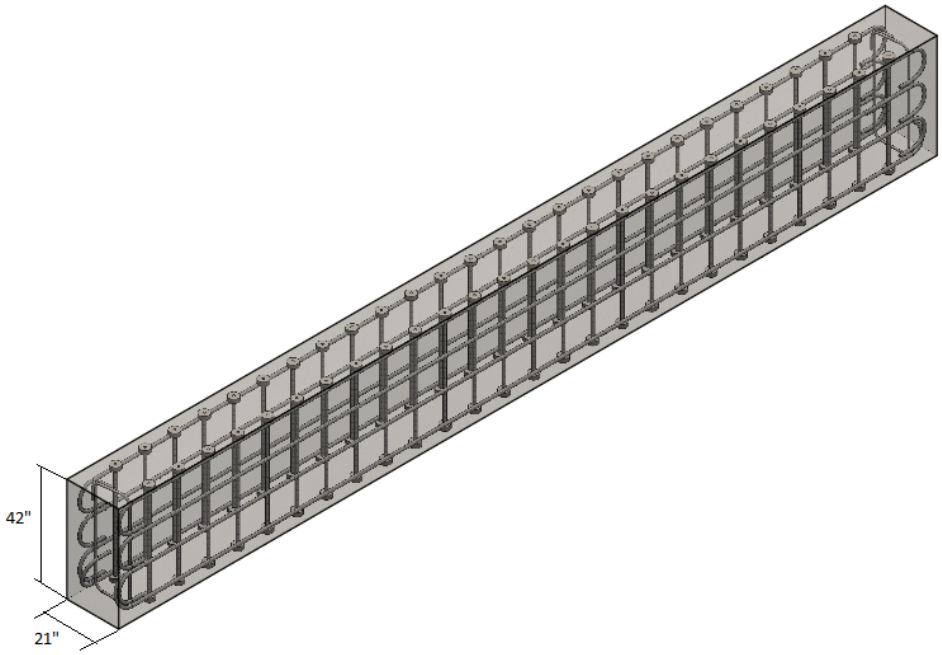

Figure 3-2: Specimen Dimensions and Reinforcement Layout

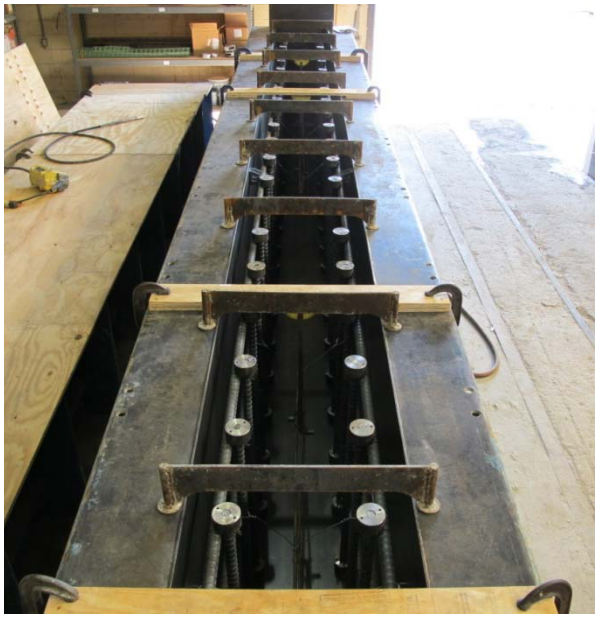

Figure 3-3: Prepared Formwork

As shown in Figure 3-4, the reinforcement layout formed square grids, each of which was considered a potential location for anchor installation and testing. The layout

of anchor testing locations was selected to maximize the number of possible test locations in each beam, while separating those test locations by at least the critical spacing distance and minimizing the necessary movement and flipping of the specimens.

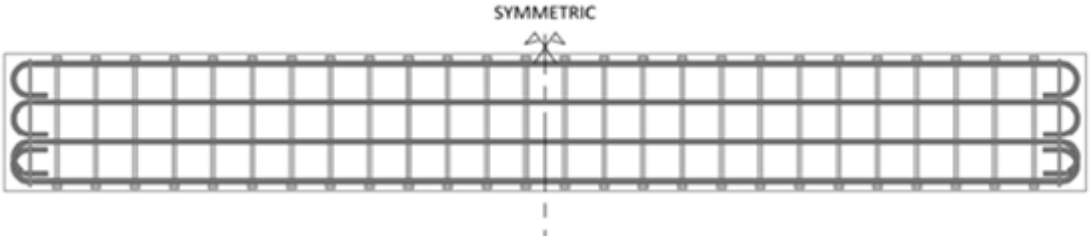

Figure 3-4: Reinforcement Layout

3.2.3 Concrete Casting

To reduce the equipment and personnel required to mix the concrete and cast the specimens, the ¾-in. crushed limestone aggregate for the mixture was delivered to Ferguson Laboratory (FSEL) in a ready-mix truck, and the remaining mixture constituents were measured and added by staff and students at FSEL. The highly reactive Jobe-Newmann sand was added to the truck by weight using a concrete bucket. The NaOH-enriched head water was measured by weight and added to the aggregates. The high-alkali Type III cement was measured by bag quantity and added to the mixture through an auger simultaneously with the water, which was measured using a flowmeter. Initially, the water was heated to 100 – 120 degrees Fahrenheit. Because this caused the concrete to set too quickly (particularly in the high ambient summer temperatures of Texas), the researchers then changed to ambient-temperature water.

Between 25 and 40 cylinders were cast along with each specimen. These were kept near their corresponding specimen under ambient conditions, and were used for compression testing up to 28 days. Immediately after each cast, the concrete specimen and cylinders were covered in a sheet of plastic for several days to prevent moisture loss while the concrete gained strength.

3.3 SPECIMEN CONDITIONING

Initially, conditioning included wrapping each specimen and a soaker hose in burlap to maintain a moist environment conducive for the development of ASR. This configuration is referred to as the "temporary conditioning location." A permanent structure, referred to as the "environmental conditioning facility" and pictured in Figure 3-5, was constructed by the researchers to store all specimens at 100% relative humidity. The anchor specimens were each arranged on 8- x 8-in. wooden blocks at approximately 3-foot spacing, for easy forklift access. The combination of the environmental curing facility and the improved specimen configuration improved control of environmental conditions and allowed access to the specimen surfaces previously obstructed by burlap.

Figure 3-5: Environmental Conditioning Facility with Open Sidewalls

The 100% relative humidity was maintained by closing all side and end walls of the facility while constantly running two foggers. The foggers were initially placed to the side of the specimens, but were replaced by overhead foggers to distribute water more evenly among the specimens. The environmental conditioning facility was used to subject the specimens to repeated cycles of one to two weeks of 100% relative humidity followed by one to two weeks of ambient relative humidity. The lengths of individual wet and dry exposures were adjusted to account for periods of freezing temperatures, movement of specimens, measurements, concrete coring, and other ad-hoc events. The temperature in the environmental conditioning facility was monitored but not controlled.

3.4 SPECIMEN MONITORING FOR GROWTH OF ASR

For this test program, ASR was monitored using a comprehensive crack index (CCI) as proposed by Fournier et al. (2010). The CCI was selected because it is simple, structure-independent, and clearly associated with the expansion experienced at the unrestrained surface of a confined member. Because the anchors are installed primarily in the cover concrete, the CCI is representative of the concrete condition most relevant to the failure mechanism.

The CCI was calculated by summing crack widths along the lines of a grid made up of 10-inch squares (Figure 3-6) and dividing by the total length of the lines. Cracks greater than or equal to 0.05 mm in width were measured and recorded. CCI measurements were recorded monthly for the first 3-12 months to establish an anticipated growth rate, and then recorded every 4th month. The CCI typically increased during the first year and then remained constant. Once the CCI stopped increasing, an official CCI measurement was required only at the time of testing.

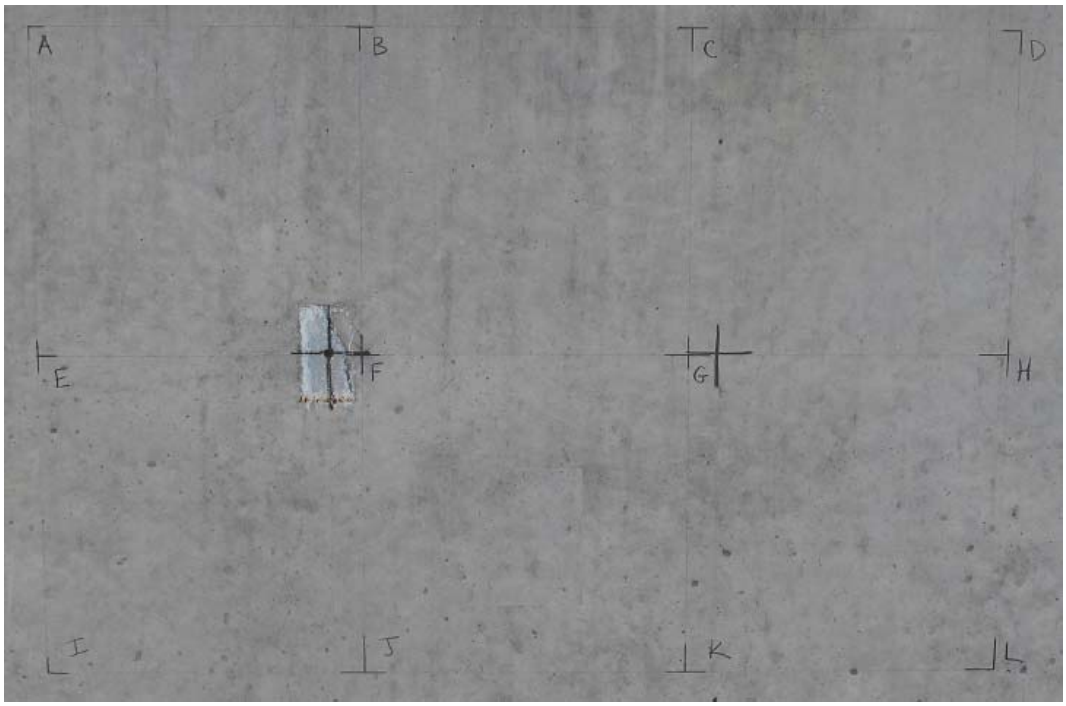

Figure 3-6: Grid for CCI Measurements

3.5 SELECTION OF ANCHORS

Wedge-type expansion anchors and undercut anchors were selected because those anchors are often found in existing structures exhibiting ASR deterioration. The diameters and embedment depths selected are typical for such anchors. Dimensions of wedge-type expansion anchors are shown in Figure 3-7. Dimensions of undercut anchors are shown in Figure 3-8. Those figures provide the embedment depths, diameters, and reference name for each anchor. In each reference name, the letter denotes the anchor type, and the sequential numbering denotes the corresponding embedment depth and diameter for each anchor. Additional details on each anchor type are provided in the following sections.

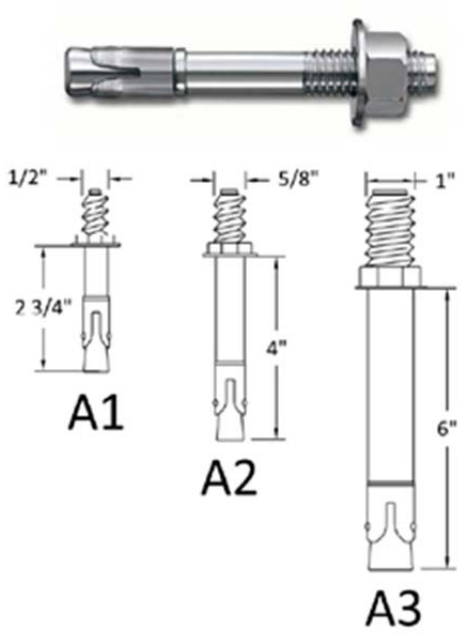

Figure 3-7: Embedment Depths of Selected Expansion Anchor

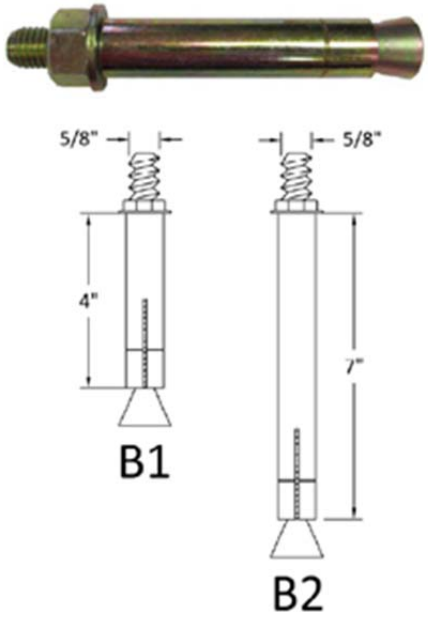

Figure 3-8: Embedment Depths of Selected Undercut Anchor

3.5.1 Installation Procedure for Torque-Controlled, Wedge-Type Expansion Anchors

Torque-controlled, wedge-type expansion anchors are installed using the following steps, shown in Figure 3-9 through Figure 3-14. A hole is first drilled into the concrete to the specified embedment depth plus the anchor diameter. The anchor is then hammered completely into that hole. Finally, a plate, a washer, and a nut are threaded onto the end of the anchor and the required torque is applied to the nut to expand the anchor against the sides of the hole.

Figure 3-9: Setting Drill Depth and Drilling Hole for Installation of Wedge Anchor

Figure 3-10: Confirming Hole Depth using Digital Calipers for Installation of Wedge Anchor

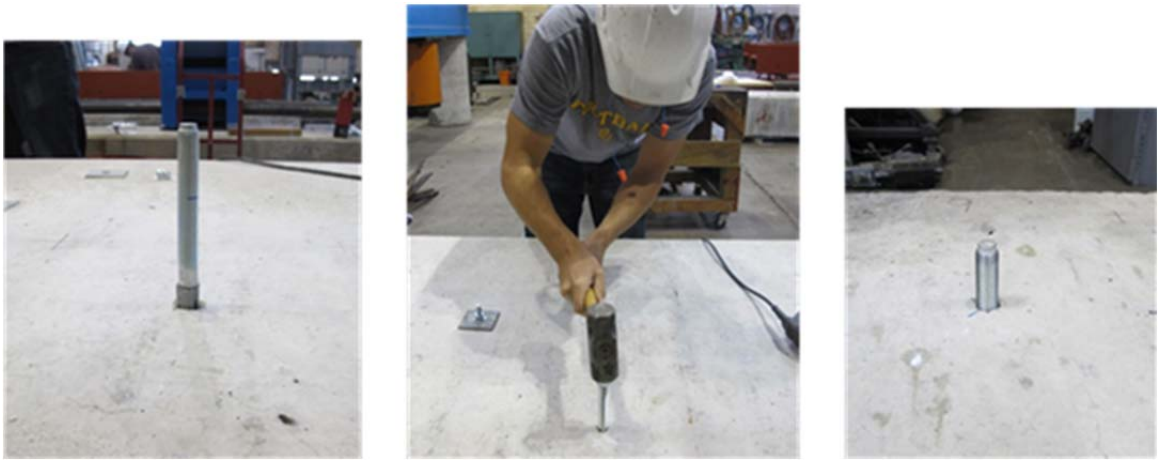

Figure 3-11: Inserting Wedge Anchor into Hole

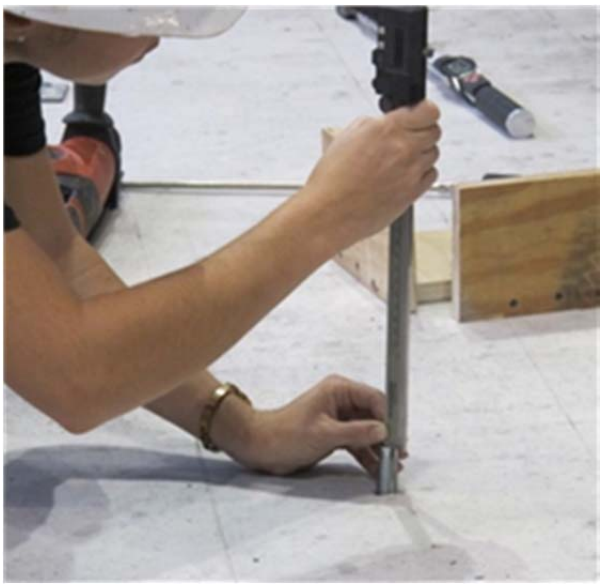

Figure 3-12: Confirming Embedment Depth of Wedge Anchor

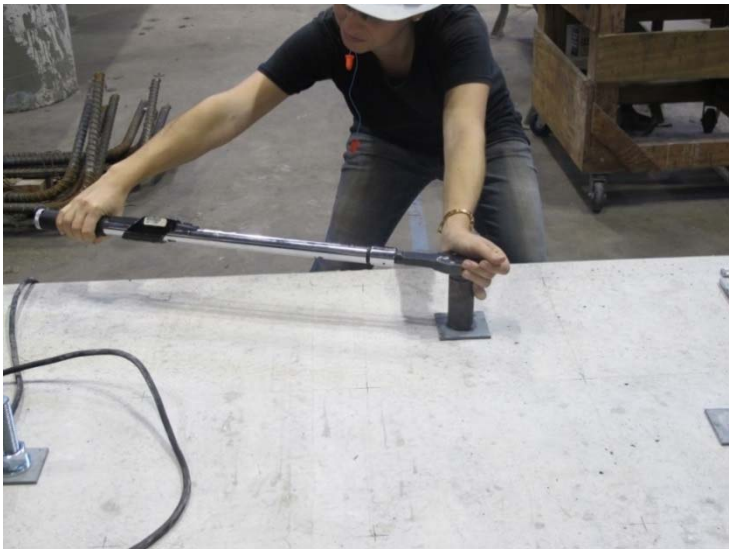

Figure 3-13: Applying Specified Torque to Set Wedge Anchor

Figure 3-14: Confirming Proper Embedment Depth of Wedge Anchor

Typical variations in depths of drilled holes, installation depths, and perpendicularity of the anchor with respect to the concrete surface have minimal impact on the tensile capacity or anchor behavior (Eligehausen and Balogh 1995). Nevertheless, for this research project, to enhance the validity of the test data, strict tolerance requirements were imposed on the depth of the drilled hole, the actual installation depth, the perpendicularity of the anchor, and the applied torque.

3.5.2 Installation Procedure for Undercut Anchors

The undercut anchor studied here was installed using tools provided by the anchor manufacturer, and following the sequence shown in Figure 3-15 and Figure 3-16. A hole is drilled into the concrete to the required embedment depth plus one inch. A special tool is used to undercut the bottom of the hole at the required depth. The anchor is then set by a manufacturer-provided setting tool and a plate, washer, and nut are threaded onto the end of the bolt. The nut is tightened to the manufacturer-specified torque, so that the anchor bears against the undercut portion of the concrete.

Figure 3-15: Undercutting the Drilled Hole

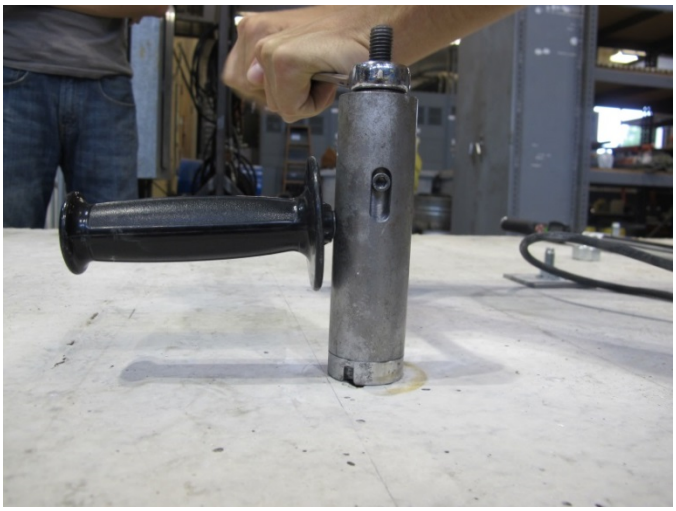

Figure 3-16: Using Setting Tool to Set Undercut Anchor

Because the manufacturer-provided tools are designed to ensure proper installation, the tolerances for installation depth of undercut anchors were not as rigorous as for

expansion anchors. Strict tolerances were applied on the installation of undercut anchors with respect to the depth of the drilled hole, the installation depth, the perpendicularity of the anchor, and the required installation torque.

3.6 DESCRIPTION OF ANCHOR TESTS

Anchors were tested in unconfined static tension to determine the influence of ASR-affected concrete on the tensile capacity and load-displacement behavior of wedge-type expansion anchors and undercut anchors.

3.6.1 Test Setup for Unconfined Anchor Tests

For the unconfined anchor tests conducted here, a smaller aluminum tripod (Figure 3-17), was used for anchors with smaller embedment depths (A1, A2, and B1), and a larger steel tripod (Figure 3-18) was used for anchors with larger embedment depths (A3 and B2). Each tripod consisted of three legs with feet bearing against the concrete and a plate welded to the top of the frame. The plate allowed the hydraulic ram to be centered about a threaded rod inserted through the middle of the tripod and attached to the anchor by a high-strength coupler. This design was intended to ensure concentric loading along the axis of the anchor.

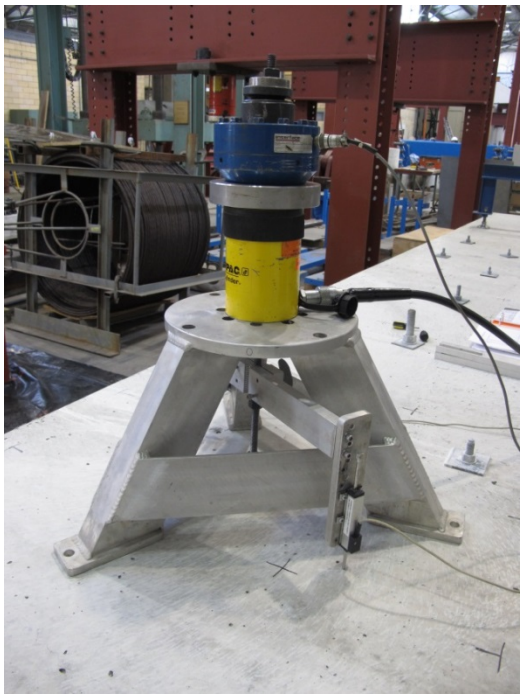

Figure 3-17: Unconfined Test Setup with Smaller Aluminum Tripod

Figure 3-18: Unconfined Test Setup with Larger Steel Tripod

The test setup for the smaller tripod, from bottom to top, included a center-hole hydraulic ram sitting on the tripod, load cell, hemispherical head, plate, washer, and nut. The tripod and all subsequent equipment were oriented concentrically about a threaded rod coupled to the anchor shaft for testing. In the setup using the larger tripod, the concentric alignment was maintained using adjustable feet on the base of each leg of the tripod, rather than a hemispherical head.

3.6.2 Testing Protocol and Instrumentation

The testing protocol was taken from ACI 355.2. Load was applied by a hydraulic hand pump attached to the hydraulic ram, at a rate set so that each test took at least one minute before failure. Testing was terminated when one of four failure criteria was met: steel fracture; concrete cone breakout; 1-inch displacement (a serviceability limit); or a 30% decrease in load. The criterion of 30% decrease in load was adopted for two reasons. First, the anchor was unlikely to regain or surpass its previously reached load capacity after this point; and second, stopping the test at this point avoided the subsequent formation of very large surface breakout regions, thereby conserving concrete in adjacent grid locations for future tests.

During the anchor tests, applied tension was measured by a load cell, and confirmed by a pressure transducer. Displacement was measured by two linear potentiometers, co-planar with the threaded rod coupled to the anchor, and attached to the rod through a machined fixture which allowed them to bear outside of the idealized projected breakout body for each anchor.

3.6.3 Data Acquisition

Data was collected by a load cell, pressure transducer, and linear potentiometers. Annual calibration verified the accuracy of the load cells and linear potentiometers. The data collection software used was LabView® by National Instruments.

Data was recorded at approximately 0.5 second intervals. The load and displacement data was converted to load-displacement curves. The maximum load before

failure was noted, along with the maximum displacement and the displacement at maximum load.

CHAPTER 4
Test Results

4.1 OVERVIEW

This section presents typical results for static unconfined tension tests on wedge-type expansion anchors and undercut anchors. The chapter begins with a discussion of ASR damage as quantified by the Comprehensive Crack Index, or CCI (Section 4.2). It proceeds with a description of the normalization process for breakout capacities (Section 4.3) and a definition of failure for anchor tests (Section 4.4). The test results (Sections 4.5, 4.6, and 4.7) are presented by Anchor (A1, A2, A3, B1, and B2) for each type of test (control, pre-ASR, and post-ASR).

4.2 MEASURED ASR DAMAGE

ASR damage is presented as a CCI measurement for each face of a specimen. A lower CCI indicates less visible cracking on the surface of the concrete and consequently less severe ASR deterioration.

4.2.1 CCI Results for Control Specimen

The control specimen was stored indoors at FSEL, and was subjected only to ambient humidity and temperature variations. As shown in Table 4-1, the CCI results for the two faces of the control specimen were 0.22 and 0.15 mm/m, indicating very early development of ASR, even without intentional conditioning to accelerate ASR deterioration. However, this level of expansion, represented by CCI measurements, is well below the expansion limits set by ASTM C227 to identify aggregates capable of harmful reactivity (Swamy and Al-Asali 1988).

Table 4-1: Summary of CCI Results

Specimen	CCI (mm/m)	
	Side 1	Side 2
Control	0.22	0.15
Post-ASR	1.29	1.00
Post-ASR	1.31	1.18
Pre-ASR	0.91	1.40

4.2.2 CCI Results for ASR-Affected Specimens

As shown in Table 4-1, the CCI results for the post-ASR specimen were 1.29, 1.00, 1.31 and 1.18 mm/m, respectively, on each face of the specimen. The additional CCI values are a result of using two smaller specimens as post-ASR specimens. The CCI results for the pre-ASR specimen were 0.91 and 1.40 mm/m, respectively, on each face. These CCI values roughly correspond to a maximum crack width of 0.15 mm. A CCI in excess of 0.5 mm/m or crack widths greater than 0.15mm justify additional investigation into concrete behavior (Fournier et al. 2010).

4.2.3 Horizontal and Vertical Expansion

To recognize differential expansion in two directions on the surface of each specimen, the CCI measurements can be further broken down into horizontal and vertical expansion measurements, displayed in Table 4-2. The results indicate unequal expansion parallel to and perpendicular to the longitudinal reinforcing bars.

Table 4-2: CCI in Horizontal and Vertical Directions

Specimen	CCI (mm/m): Side 1		CCI (mm/m): Side 2	
	Horizontal	Vertical	Horizontal	Vertical
Post-ASR Installed	1.68	0.86	1.33	0.61
Post-ASR Installed	1.64	0.93	1.49	0.83
Pre-ASR Installed	1.29	0.49	1.90	0.83

4.3 DEFINITION OF FAILURE FOR ANCHOR TESTS

Four types of failure were recognized during unconfined tensile tests:

1) Steel fracture;
2) Concrete cone breakout;
3) 1-inch displacement; and
4) 30% decrease in load.

The first three of these failure types are depicted in Figure 4-1.

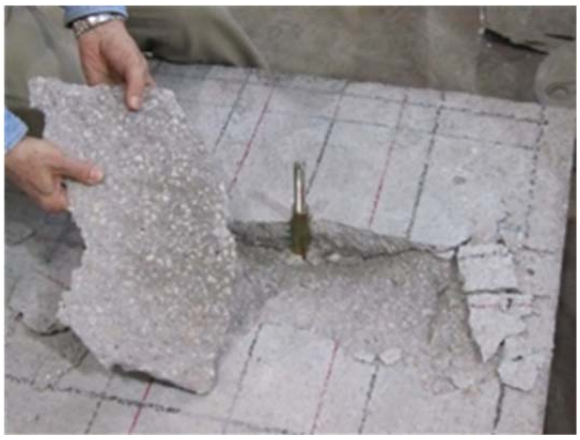

a) concrete cone breakout

b) 1-inch displacement

c) steel fracture

Figure 4-1: Photographic Depictions of Concrete Cone Breakout Failure, 1-inch Displacement, and Steel Fracture

4.4 NORMALIZATION OF ANCHOR CAPACITIES

Anchor capacities are normalized with respect to expected breakout capacity as predicted by the design equations of Appendix D of ACI 318-11. Those design equations are calibrated to produce 5% fractile values for a sample coefficient of variation of 15%. The expected breakout capacity is determined by dividing those 5% fractile values by 0.7 (DeFurio et al. 2012). The leading constant, k_c, is taken equal to 17 for post-installed anchors, and was used for the expansion anchors. The leading constant k_c is taken equal to 24 for cast-in place anchors, and was used for the undercut anchors.

This normalization allows for the comparison of anchors across embedment depths and concrete strengths. Normalized results greater than 1.0 indicate anchor performance above the expected average value, while normalized results less than 1.0 indicate anchor performance below the expected average value.

4.5 Unconfined (Breakout) Tests of Expansion and Undercut Anchors in ASR-Affected Concrete

In total, 85 anchors were tested. Anchors were installed in control specimens, pre-ASR specimens; and post-ASR specimens. The tests are referred to respectively as control tests, pre-ASR tests, and post-ASR tests. Altogether, there were 30 control tests, 30 pre-ASR tests, and 25 post-ASR tests.

Expansion anchors accounted for 51 of these tests. Of the expansion anchor tests; 18 were control tests, 18 were pre-ASR tests, and 15 were post-ASR tests. Undercut anchors accounted for 34 anchor tests. Of these, 12 were control tests, 12 were pre-ASR tests, and 10 were post-ASR tests. At least five tests in each specimen type were conducted for each Anchor A1, A2, A3, B1, and B2.

4.5.1 Differences between Pre-ASR and Post-ASR Tests

Because ASR normally develops after anchor installation, the pre-ASR tests of this research program most closely represent the expected behavior of anchors in the field. Additionally, because steel relaxes over time, the inclusion of a time interval between installation and testing is more representative of field conditions. Previous literature has shown relaxation of the steel does not affect tensile capacity (Eligehausen and Balogh 1995).

Because micro-cracking is present in the concrete when the anchor is installed, post-ASR tests more closely resemble other researchers' work on anchor testing in cracked concrete

4.6 TEST RESULTS FOR EXPANSION ANCHORS

Normalized tensile capacities of expansion anchors installed in control, pre-ASR, and post-ASR concrete are presented in the following sections. The normalized capacities are plotted against the CCI of the respective specimens, followed by a typical load-displacement curve for each anchor.

4.6.1 Normalized Capacities of Expansion Anchors in Control Specimens

Normalized capacities of expansion anchors tested in control specimens are shown in Figure 4-2.

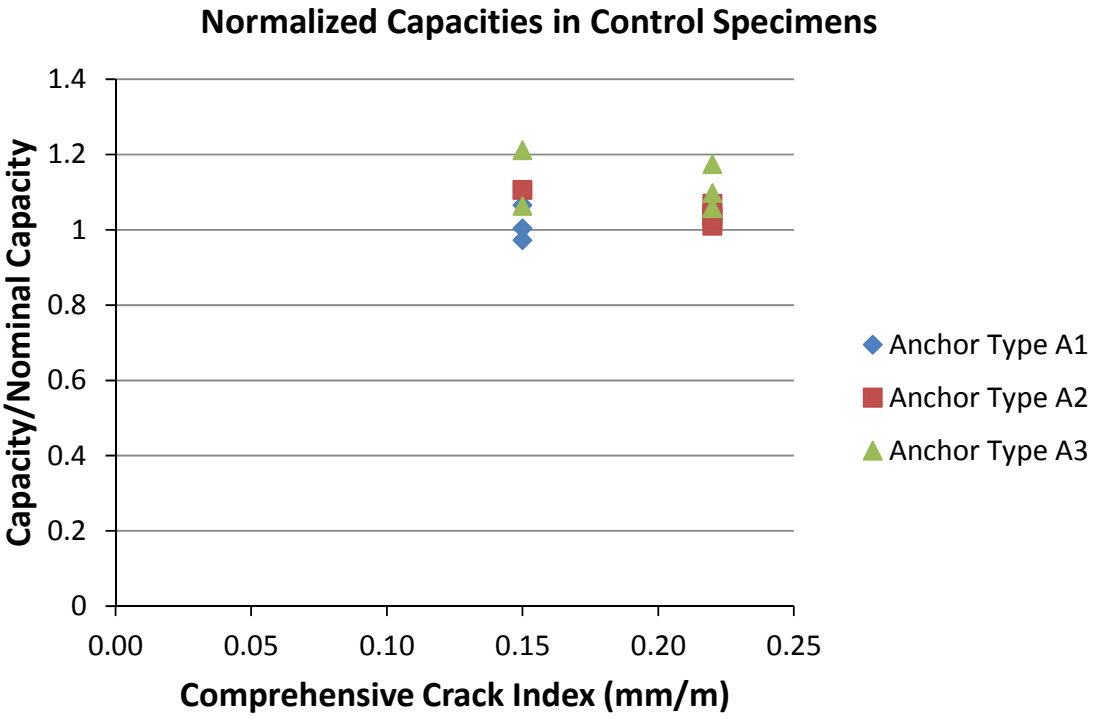

Figure 4-2: Normalized Capacities of Expansion Anchors in Control Specimens

Anchors A1 and A2 consistently failed by concrete breakout or by a 30% drop in load. Typical behavior for Anchors A1 and A2 are shown respectively in Figure 4-3 and Figure 4-4. Anchor A3 invariably failed by a 1-inch displacement. A typical load-displacement curve for Anchor A3 is shown in Figure 4-5.

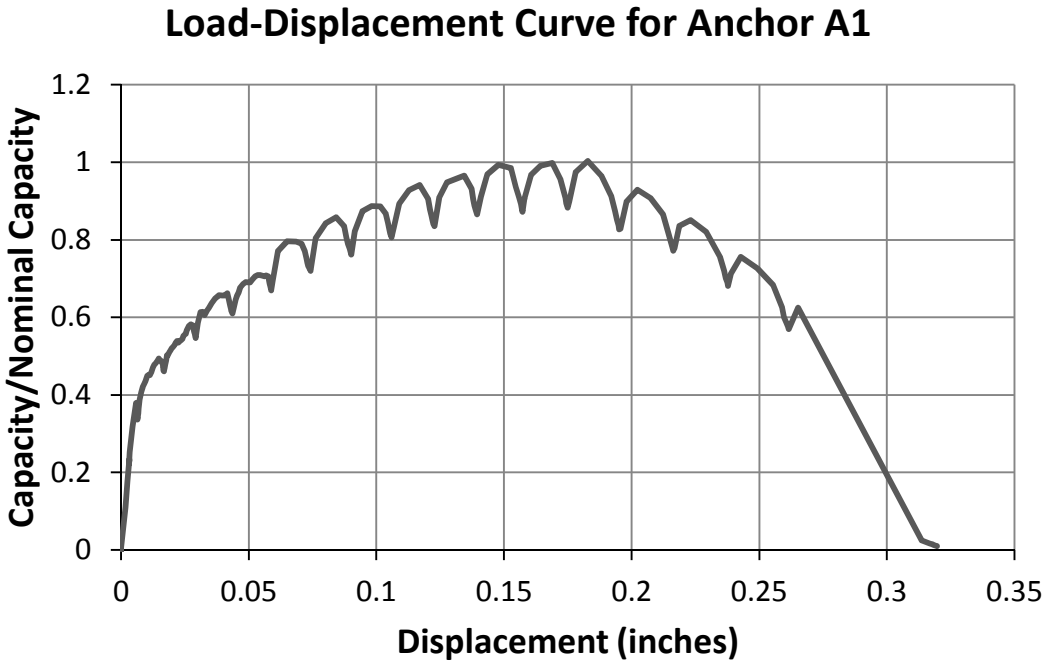

Figure 4-3: Typical Load-Displacement Behavior of Expansion Anchor A1 in Control Specimen

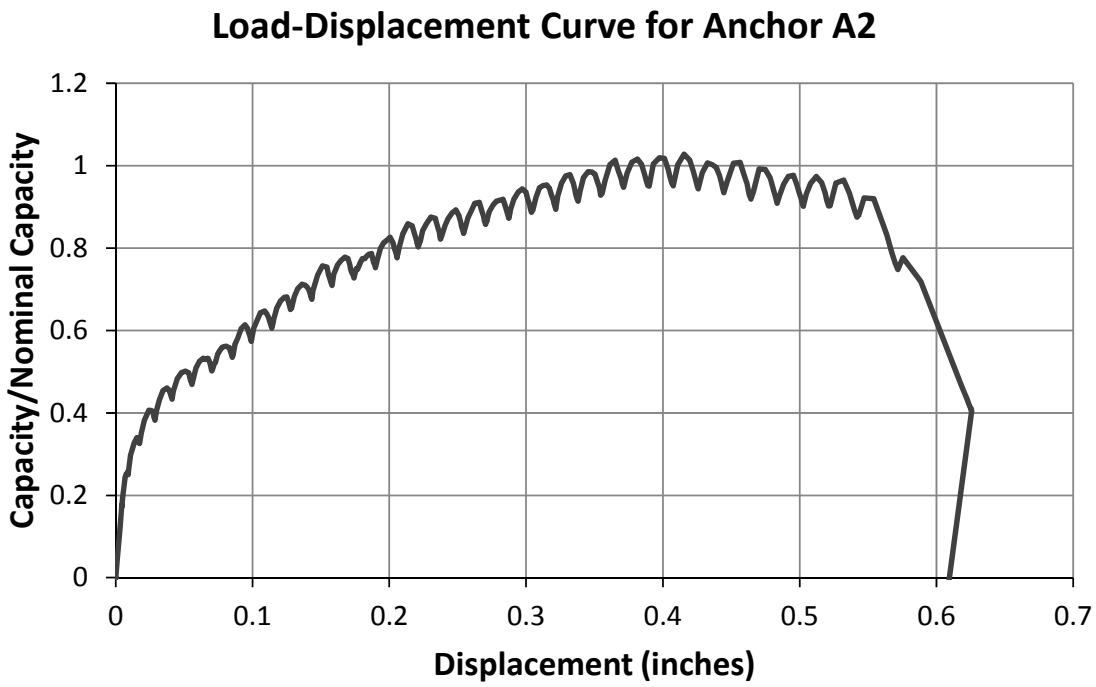

Figure 4-4: Typical Load-Displacement Behavior of Expansion Anchor A2 in Control Specimen

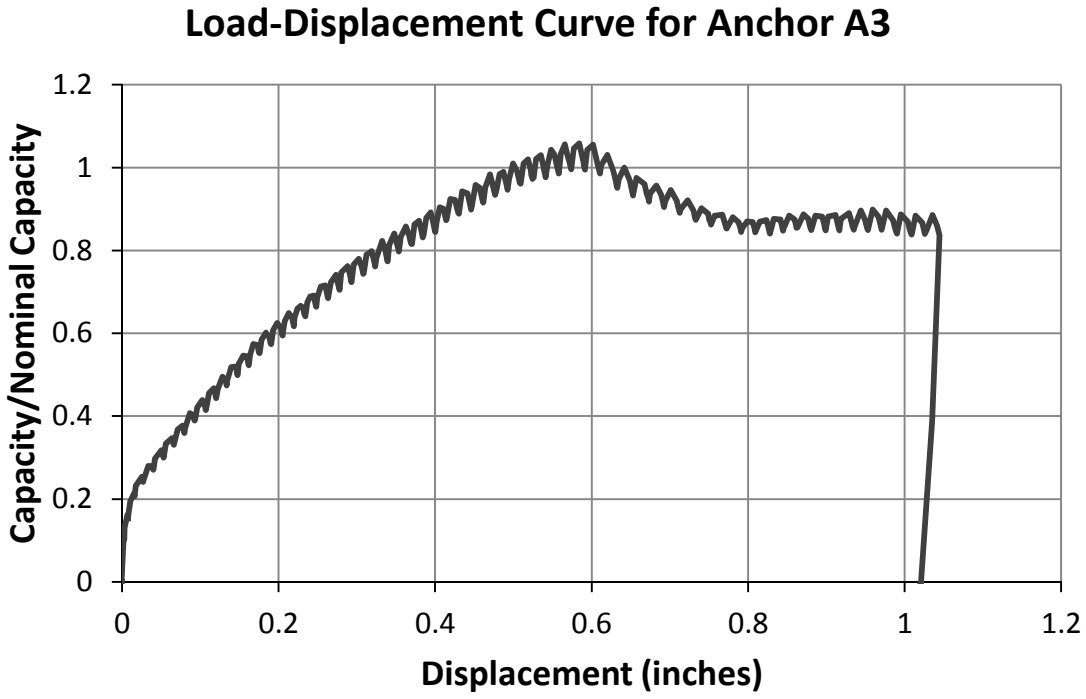

Figure 4-5: Typical Load-Displacement Behavior of Expansion Anchor A3 in Control Specimen

4.6.2 Normalized Capacities of Expansion Anchors in Pre-ASR Specimens

Normalized capacities of expansion anchors tested in pre-ASR specimens are shown in Figure 4-6. Typical load-displacement curves are shown in Figure 4-7 through Figure 4-9.

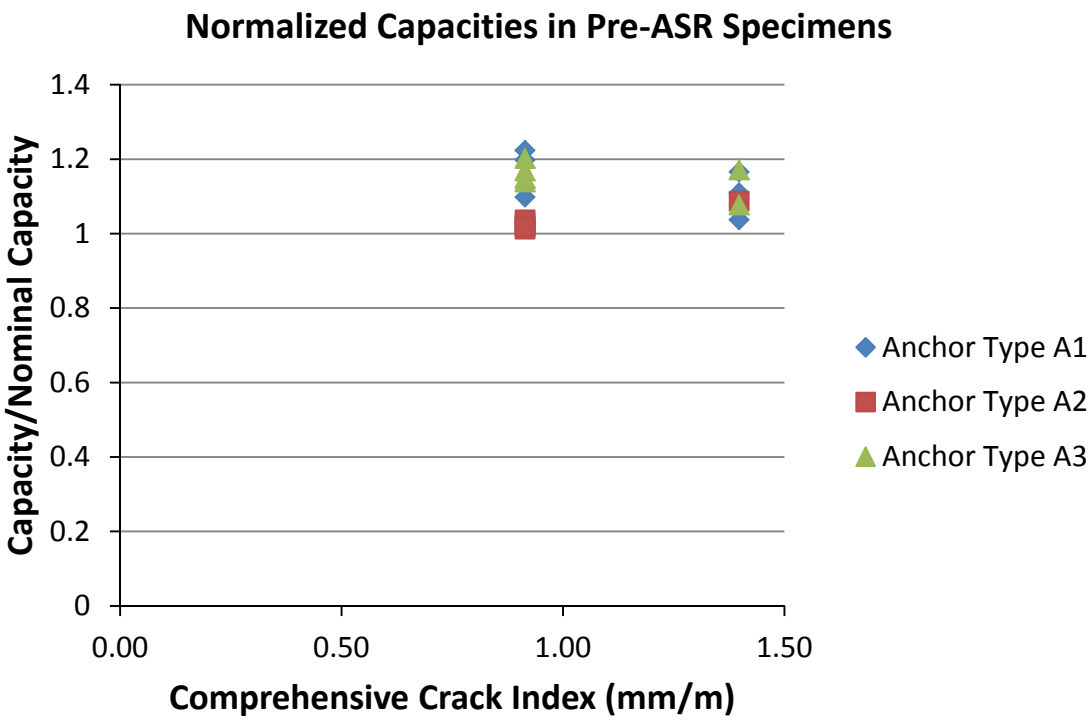

Figure 4-6: Normalized Capacities of Expansion Anchors in Pre-ASR Specimens

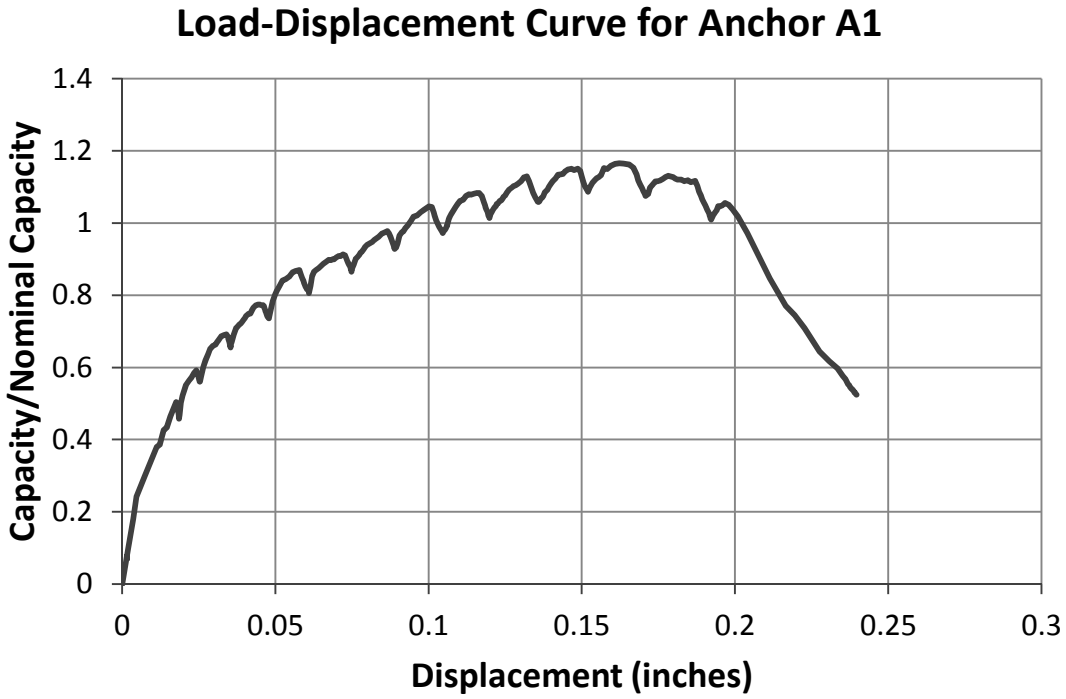

Figure 4-7: Typical Load-Displacement Behavior of Expansion Anchor A1 in Pre-ASR Specimen

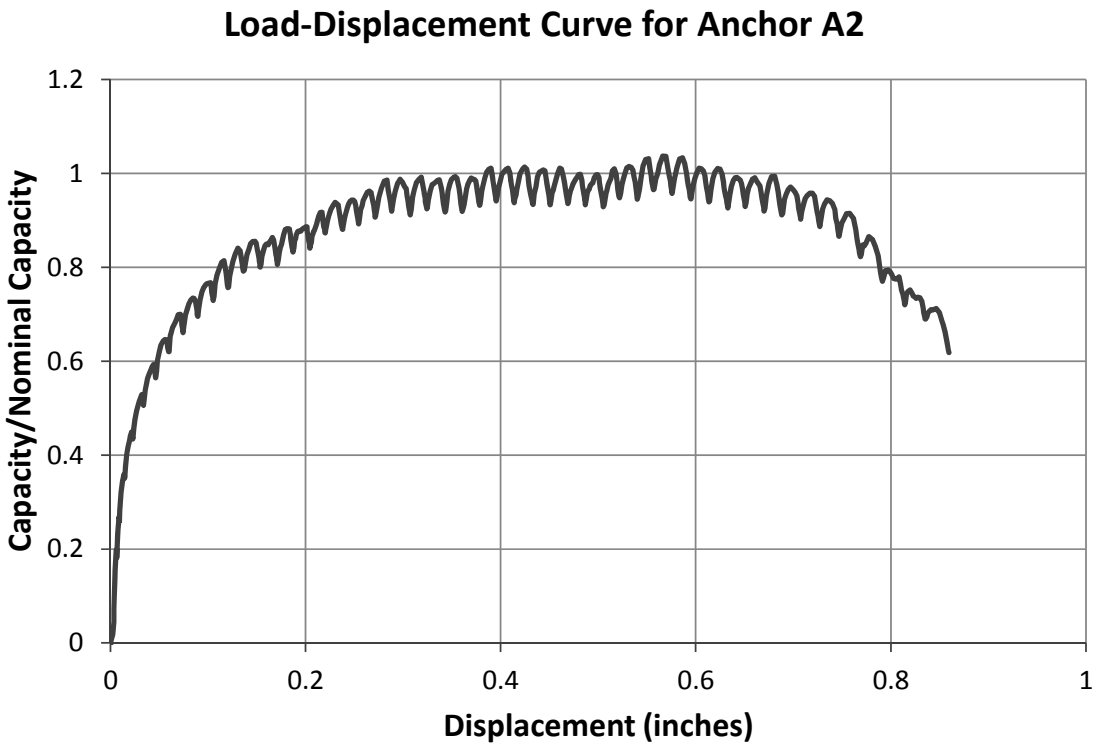

Figure 4-8: Typical Load-Displacement Behavior of Expansion Anchor A2 in Pre-ASR Specimen

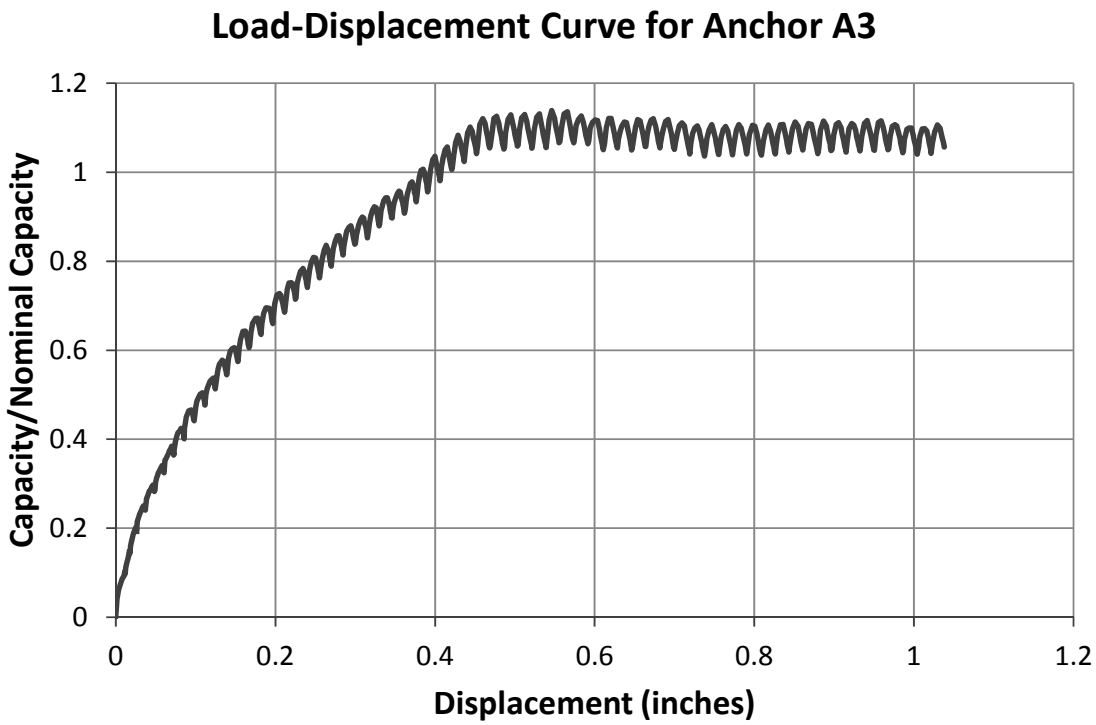

Figure 4-9: Typical Load-Displacement Behavior of Expansion Anchor A3 in Pre-ASR Specimen

4.6.3 Normalized Capacities of Expansion Anchors in Post-ASR Specimens

Normalized capacities of expansion anchors tested in post-ASR specimens are shown in Figure 4-10. Typical load-displacement curves are shown in Figure 4-11 through Figure 4-13 .

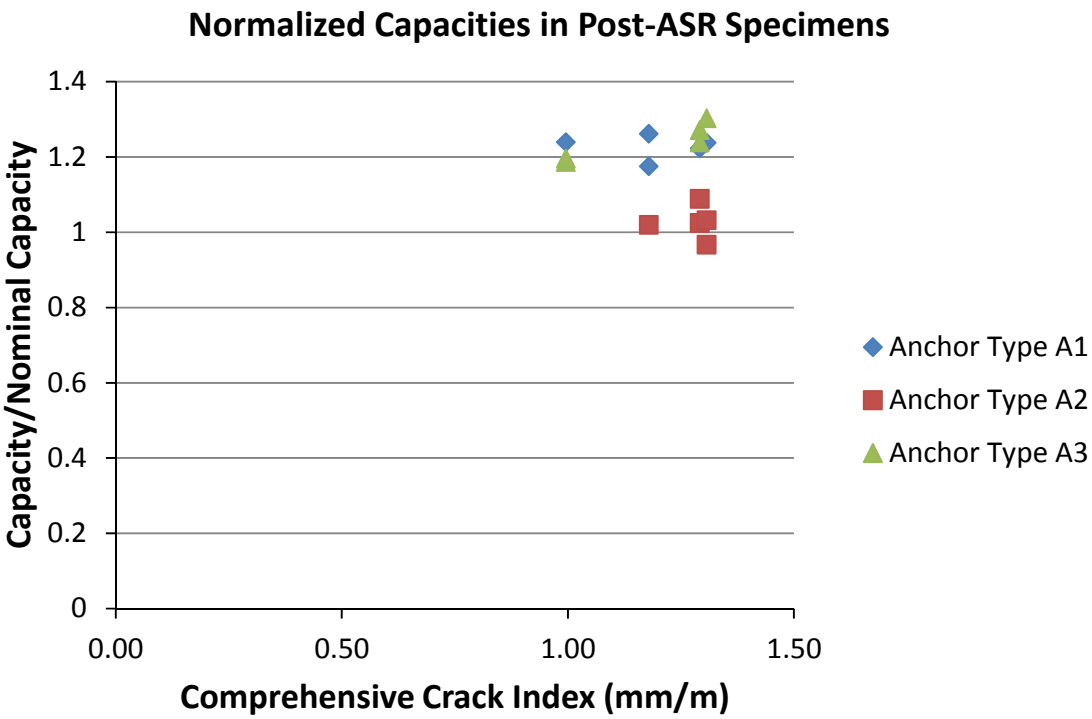

Figure 4-10: Normalized Capacities of Expansion Anchors in Post-ASR Specimens

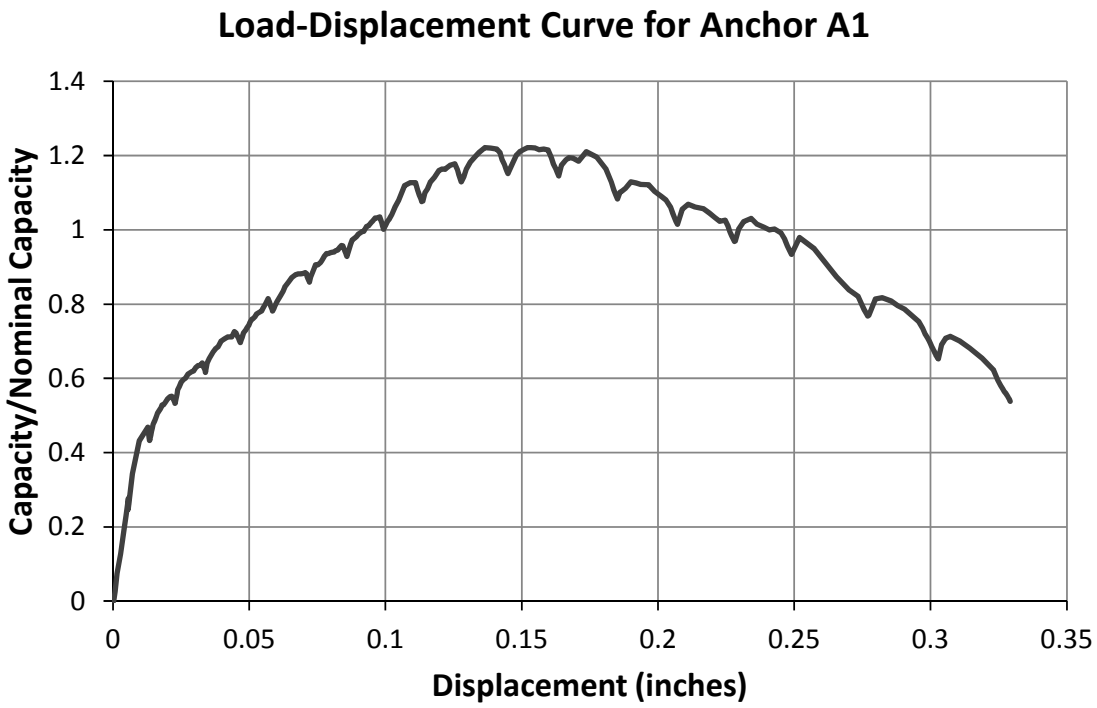

Figure 4-11: Typical Load-Displacement Behavior of Expansion Anchor A1 in Post-ASR Specimen

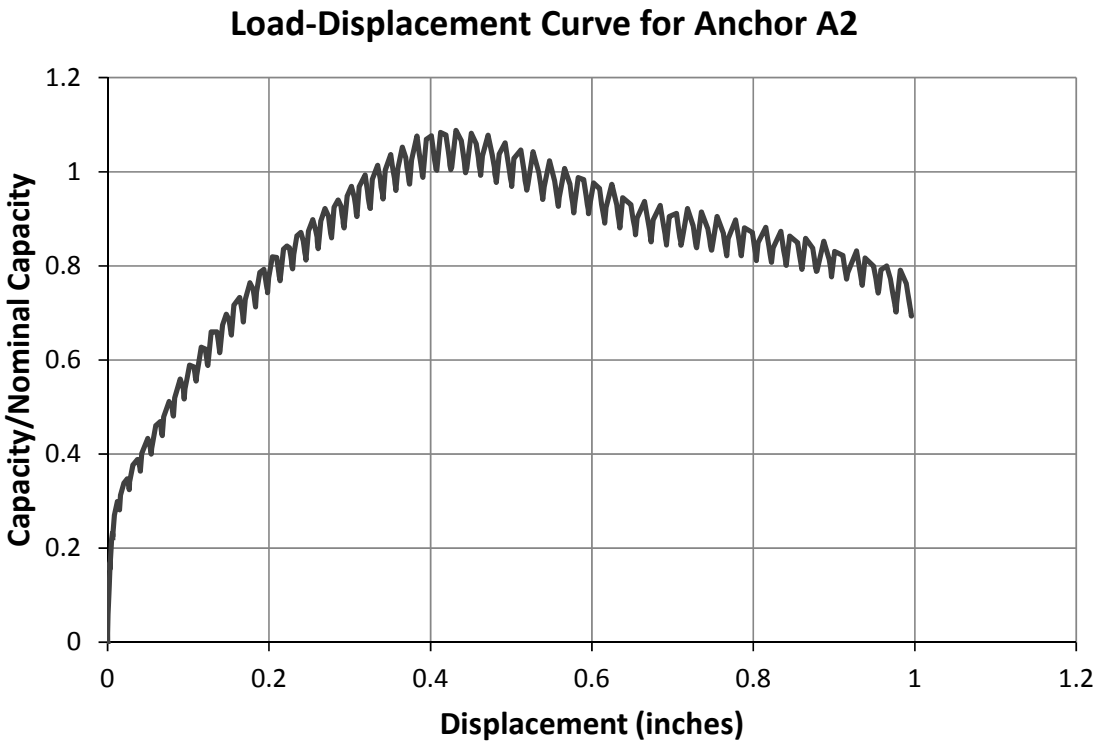

Figure 4-12: Typical Load-Displacement Behavior of Expansion Anchor A2 in Post-ASR Specimen

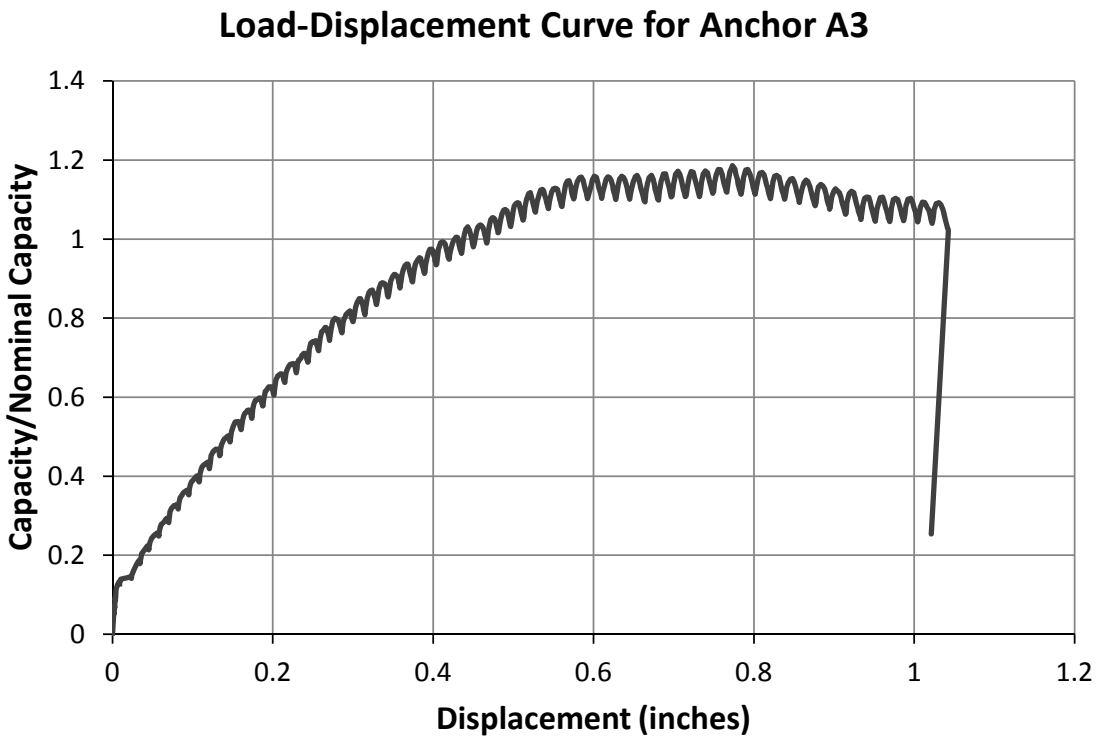

Figure 4-13: Typical Load-Displacement Behavior of Expansion Anchor A3 in Post-ASR Specimen

4.7 TEST RESULTS FOR UNDERCUT ANCHORS

Tensile test results for control, pre-ASR, and post-ASR installed undercut anchors are presented in the following section. The normalized capacities are plotted against the CCI of each respective specimen followed by a typical load-displacement curve for each anchor.

4.7.1 Normalized Capacities of Undercut Anchors in Control Specimens

Normalized capacities of undercut anchors tested in control specimens are shown in Figure 4-14.

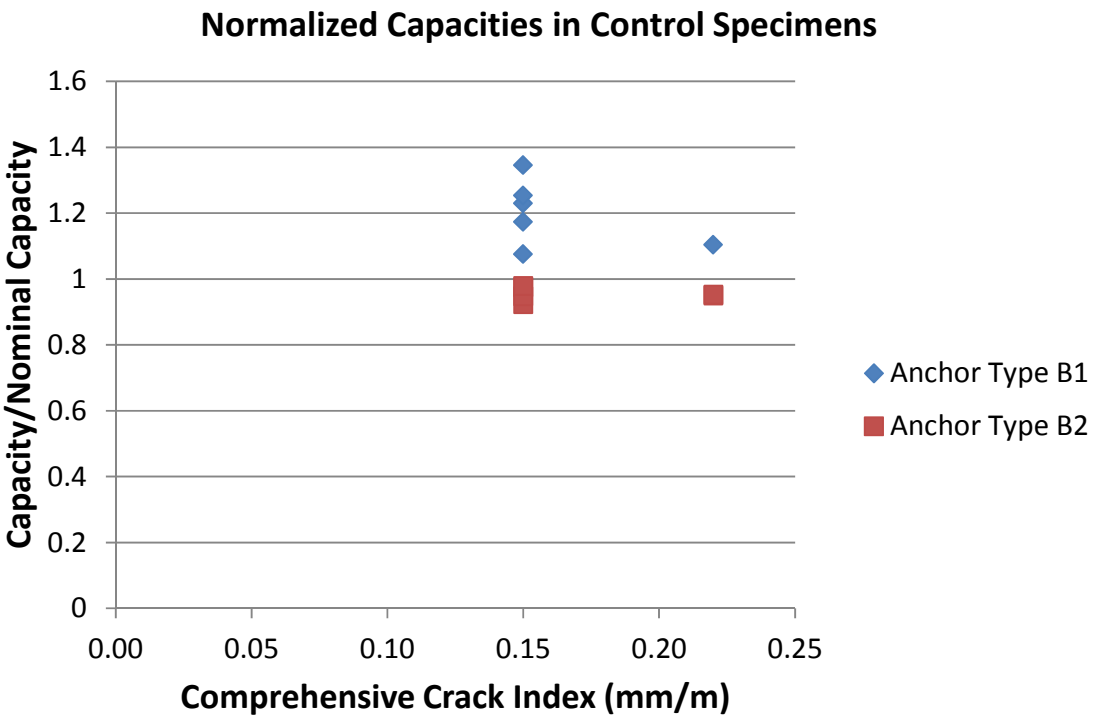

Figure 4-14: Normalized Capacities of Undercut Anchors in Control Specimens

Anchor B1 failed in concrete cone breakout or by a 30% load drop for all tests. A typical load-displacement curve for anchor B1 is shown in Figure 4-15. Anchor B2 failed in steel fracture or pullout for all tests. A typical load-displacement curve for Anchor B2 is shown in Figure 4-16.

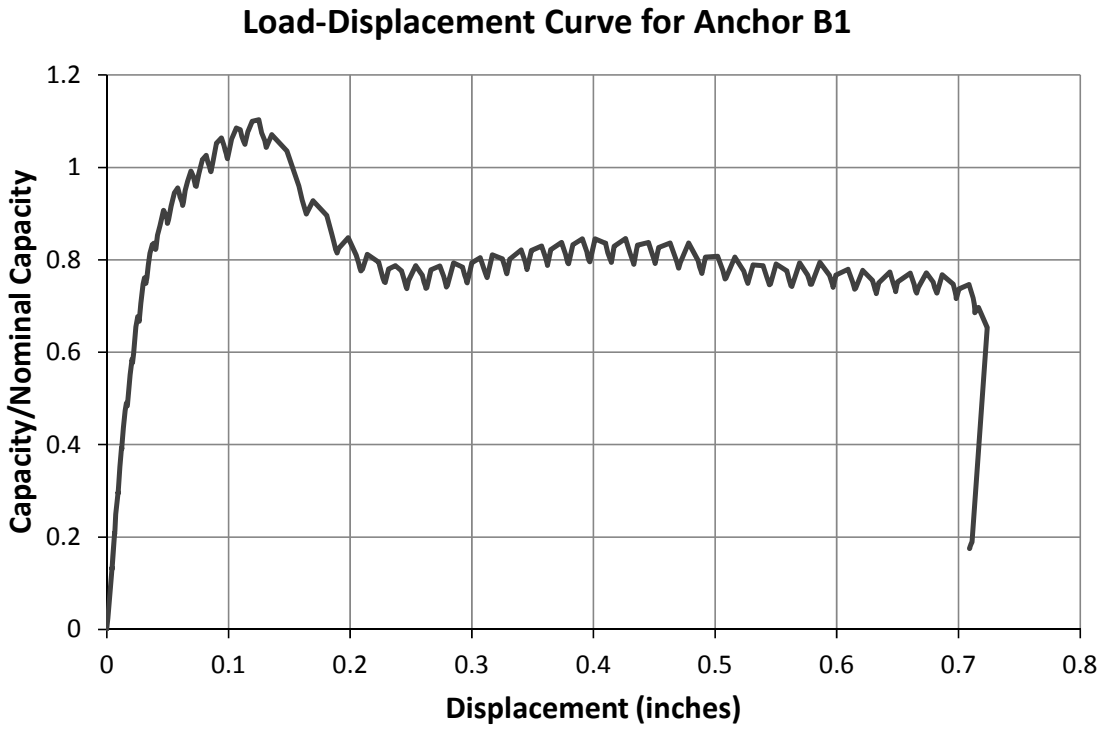

Figure 4-15: Typical Load-Displacement Behavior of Undercut Anchor B1 in Control Specimen

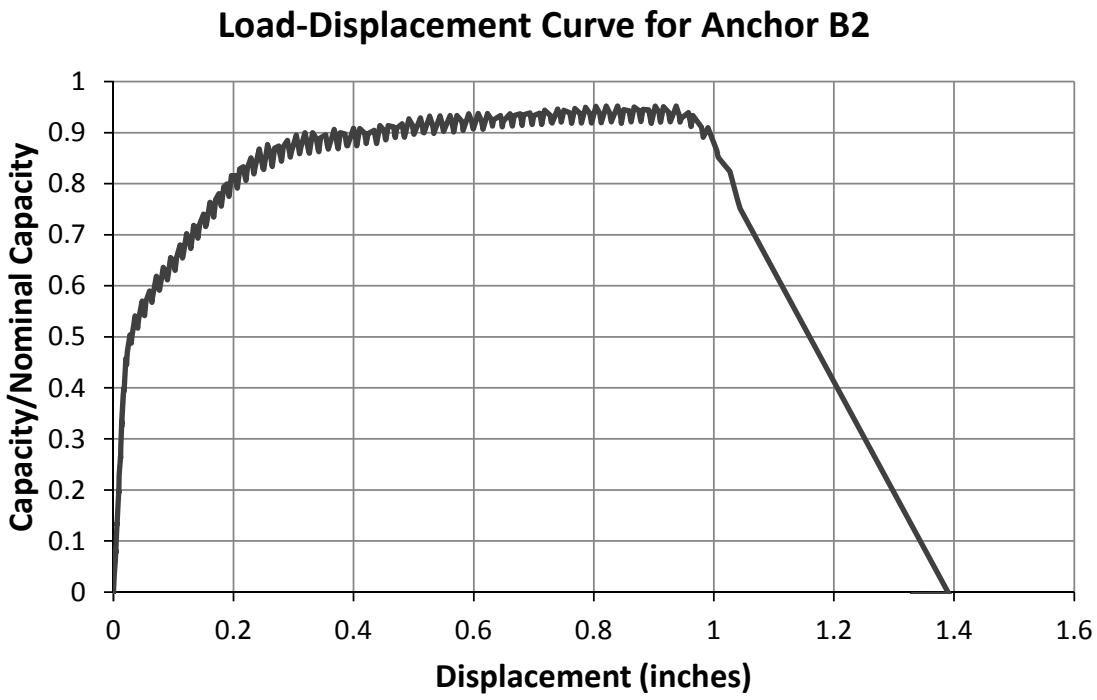

Figure 4-16: Typical Load-Displacement Behavior of Undercut Anchor B2 in Control Specimen

4.7.2 Normalized Capacities of Undercut Anchors in Pre-ASR Specimens

Normalized capacities of undercut anchors tested in pre-ASR specimens are shown in Figure 4-17. Typical load-displacement curves are shown in Figure 4-18 and Figure 4-19.

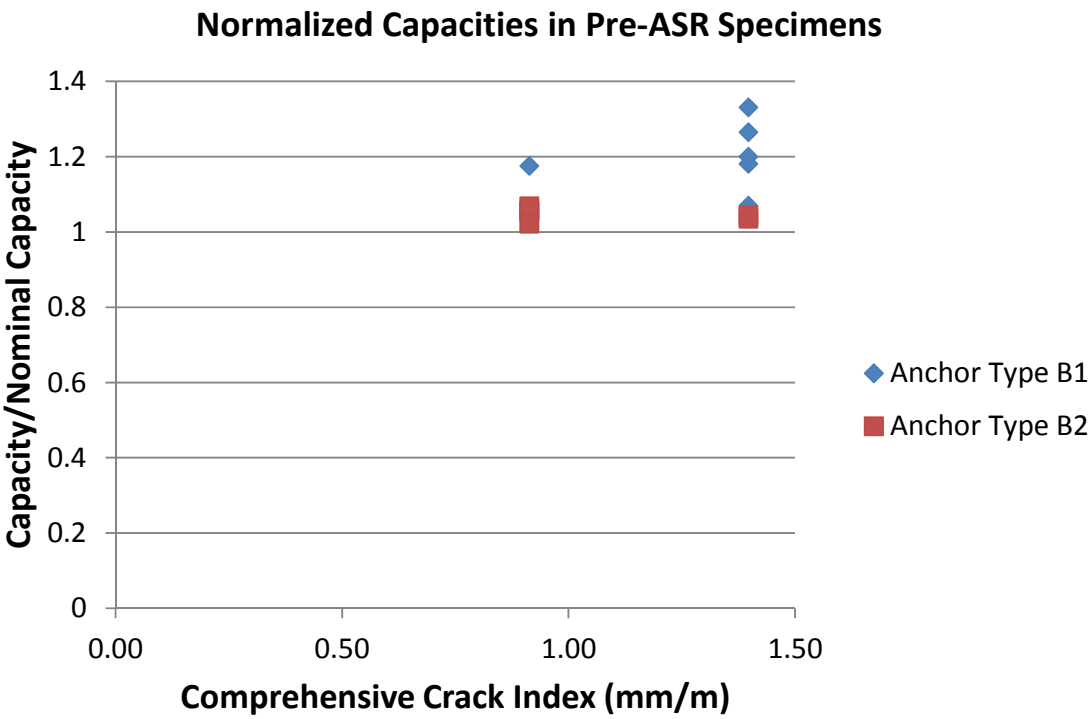

Figure 4-17: Normalized Capacities of Undercut Anchors in Pre-ASR Specimens

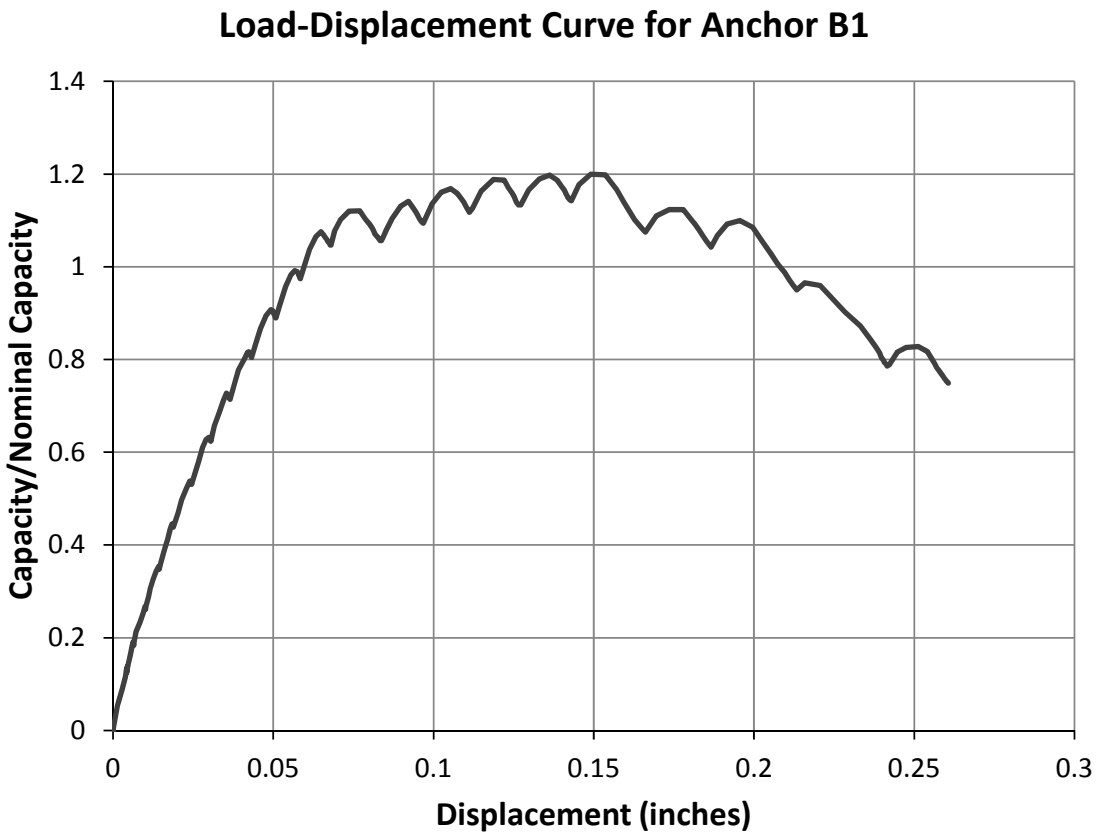

Figure 4-18: Typical Load-Displacement Behavior of Undercut Anchor B1 in Pre-ASR Specimen

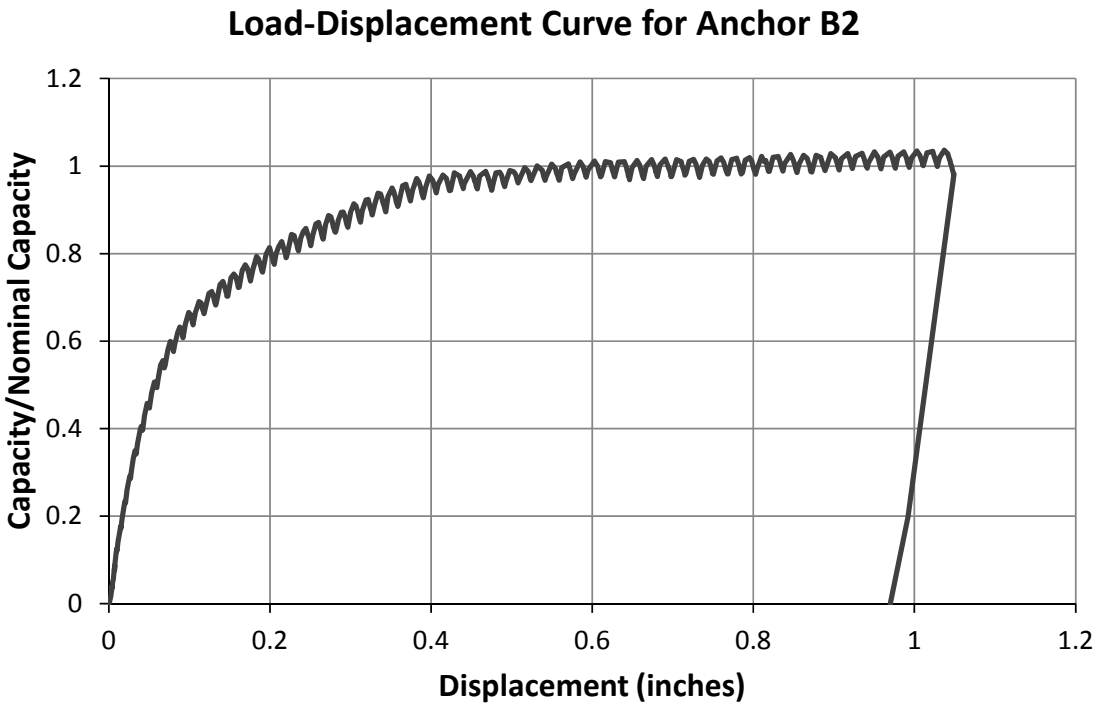

Figure 4-19: Typical Load-Displacement Behavior of Undercut Anchor B2 in Pre-ASR Specimen

4.7.3 Normalized Capacities of Undercut Anchors in Post-ASR Tests Specimens

Normalized capacities of undercut anchors tested in post-ASR specimens are shown in Figure 4-20. Typical load-displacement curves are shown in Figure 4-21 and Figure 4-22.

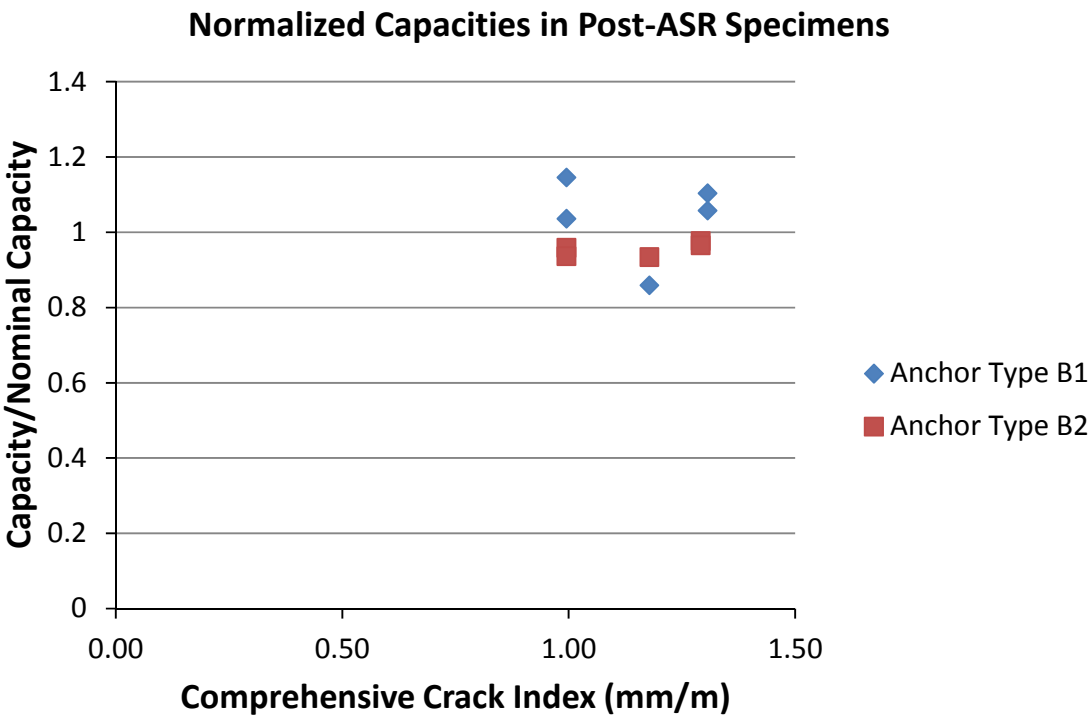

Figure 4-20: Normalized Capacities of Undercut Anchors in Post-ASR Specimens

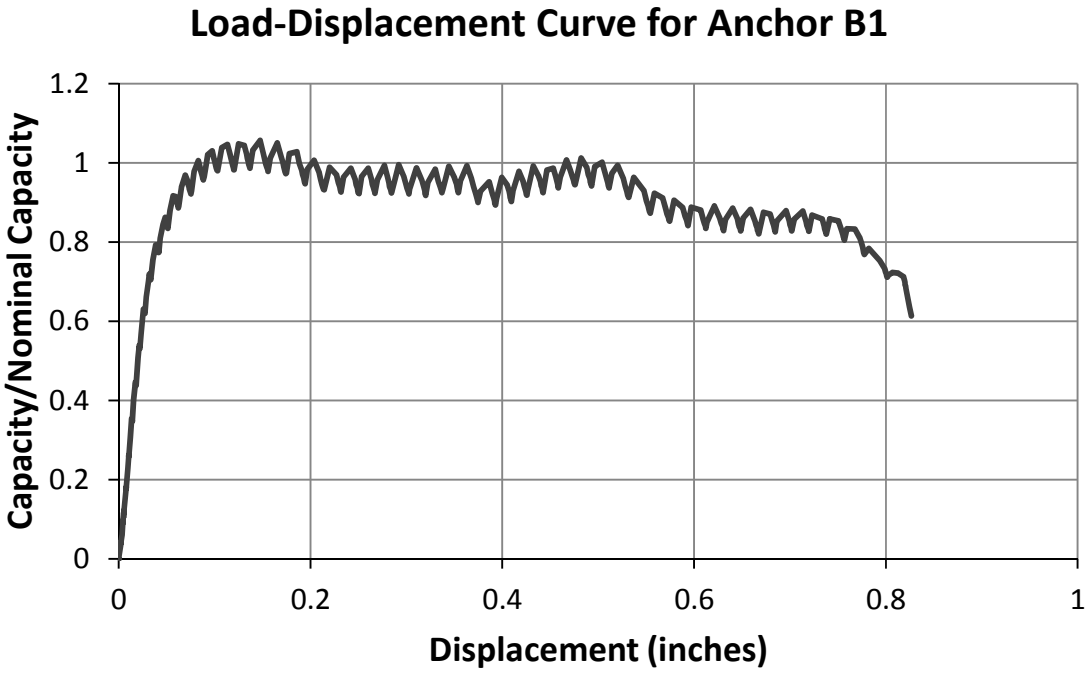

Figure 4-21: Typical Load-Displacement Behavior of Undercut Anchor B1 in Post-ASR Specimen

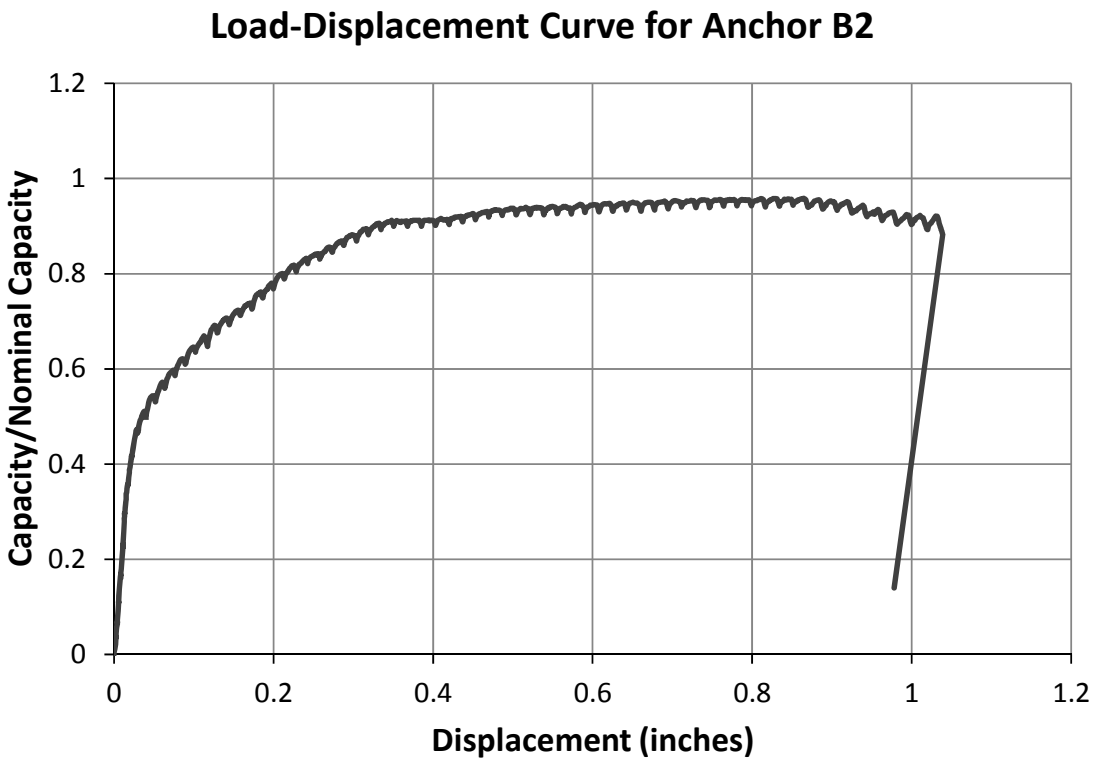

Figure 4-22: Typical Load-Displacement Behavior of Undercut Anchor B2 in Post-ASR Specimen

CHAPTER 5
Discussion of Test Results

5.1 OVERVIEW

This chapter presents a discussion of the test results (Section 5.2) for wedge-type expansion anchors and undercut anchors. Normalized capacities are plotted against both the Comprehensive Crack Index (CCI) and the nominal embedment depth. The next two sections (Sections 5.3 and 5.4) address the statistical variation of capacities for all anchors. The last section (Section 5.5) contains a discussion of the differences between the performance of expansion and undercut anchors in ASR-affected concrete.

5.2 SUMMARY OF NORMALIZED TENSILE CAPACITIES

Normalized tensile capacities are plotted against the CCI in Figure 5-1 and Figure 5-2 for expansion and undercut anchors, respectively. Normalized tensile capacities are plotted against effective embedment depth in Figure 5-3 and Figure 5-4 for expansion and undercut anchors, respectively. The latter capacities are normalized only with respect to concrete strength, not embedment depth. As expected, these plots show the capacity increasing with embedment depth. These results are compared directly to the theoretical anchor capacity as the effective embedment depth increases.

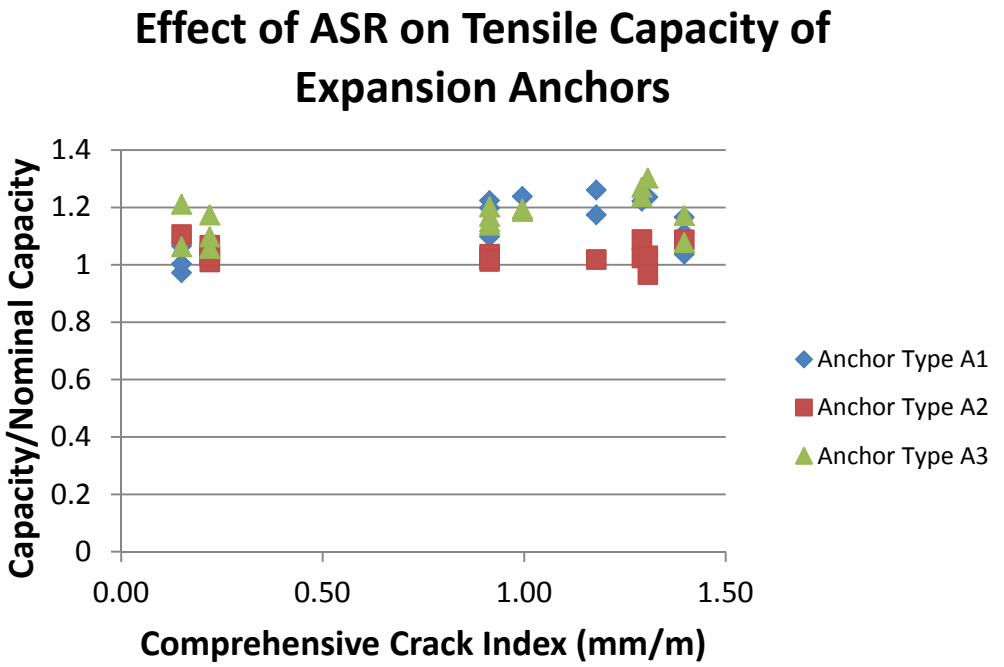

Figure 5-1: Normalized Tensile Capacities of Expansion Anchors versus CCI

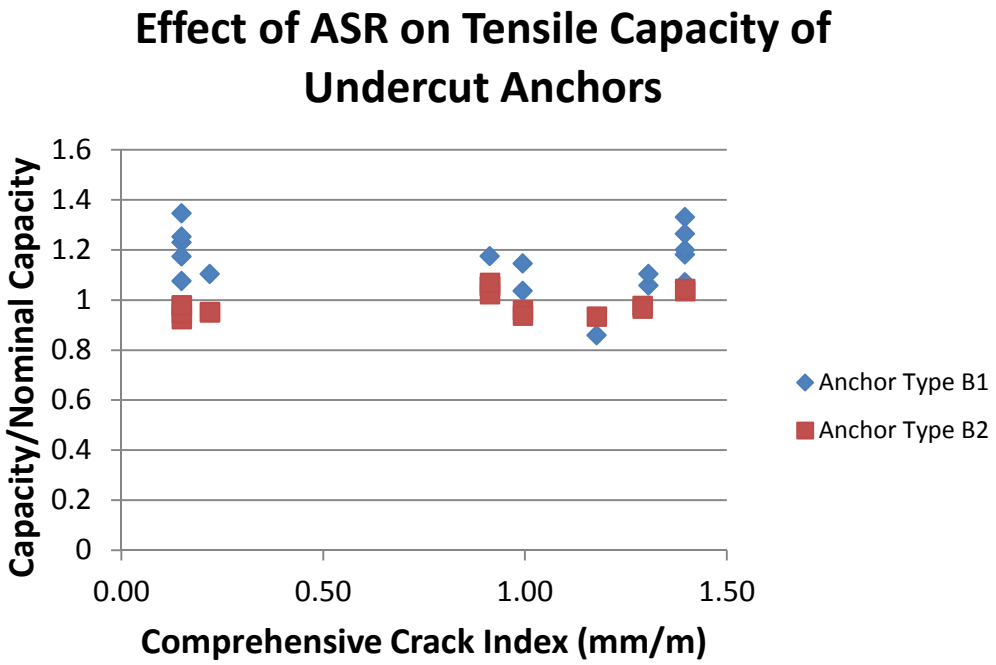

Figure 5-2: Normalized Tensile Capacities of Undercut Anchors versus CCI

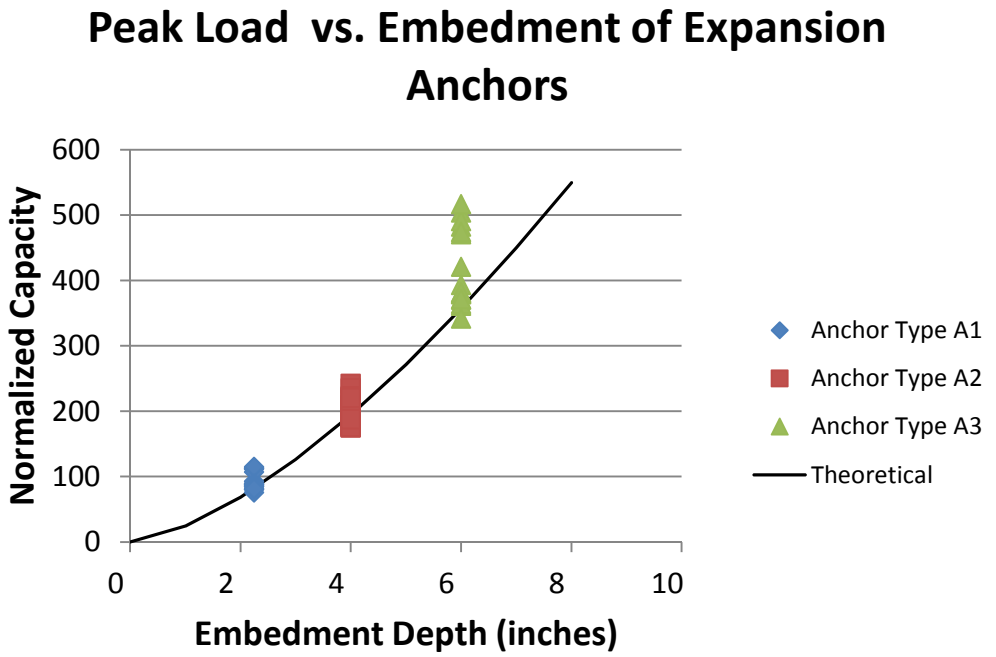

Figure 5-3: Tensile Capacities of Expansion Anchors versus Embedment Depth

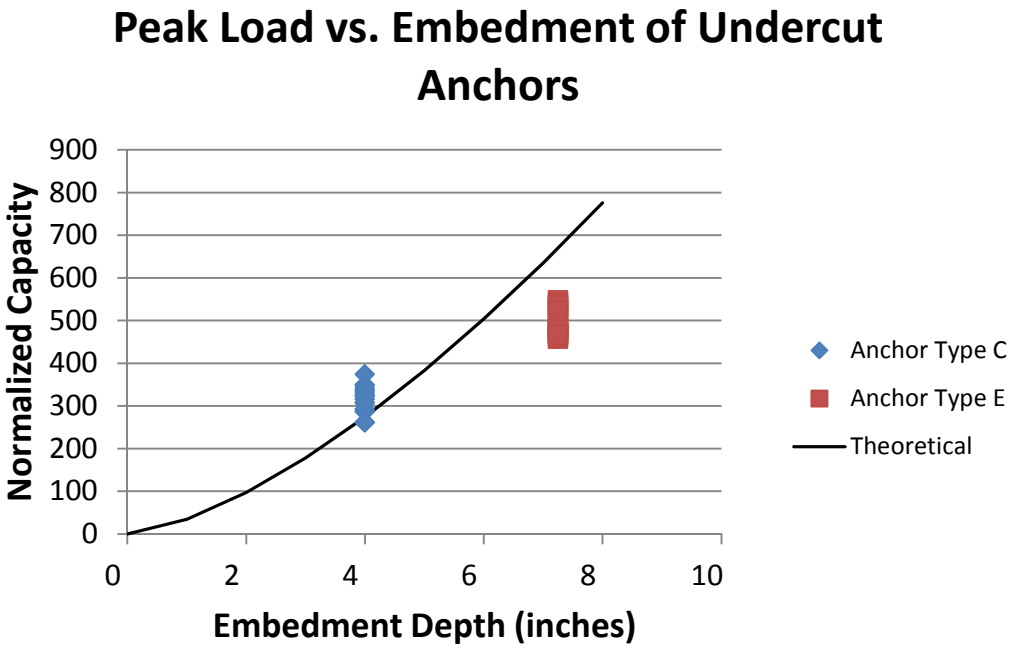

Figure 5-4: Tensile Capacities of Undercut Anchors versus Embedment Depth

5.3 STATISTICAL VARIATION OF CAPACITIES FOR EXPANSION ANCHORS

The sample sizes, mean normalized capacities, and coefficients of variation (COV) of capacities are shown in Table 5-1, Table 5-2, and Table 5-3, respectively, for each expansion anchor.

Table 5-1: Statistical Distribution of Results for Anchor A1

	Sample Size	mean (normalized capacities)	COV (capacities)
Control	6	1.03	0.034
Pre-ASR Installed Anchors/CCI =	6	1.14	0.061
Post-ASR Installed Anchors/ CCI =	5	1.23	0.026

Table 5-2: Statistical Distribution of Results for Anchor A2

	n	mean (normalized capacities)	COV (capacities)
Control	6	1.05	0.033
Pre-ASR Installed Anchors/CCI =	6	1.03	0.027
Post-ASR Installed Anchors/ CCI =	5	1.03	0.042

Table 5-3: Statistical Distribution of Results for Anchor A3

	n	mean (normalized capacities)	COV (capacities)
Control	6	1.11	0.060
Pre-ASR Installed Anchors/CCI =	6	1.15	0.037
Post-ASR Installed Anchors/ CCI =	5	1.24	0.040

For expansion anchors all normalized mean capacities are greater than 1.0. The COVs for anchors tested under this research program are smaller than the 15% COV found in the literature for anchors in cracked concrete.

A histogram of the normalized tensile capacities of Anchors A1, A2, and A3 is shown in Figure 5-5. Because there is little difference between the ratios of observed capacity to expected mean capacity for all anchors, the results are presented on a single graph. This histogram represents one distribution of the results; changing the bin size may alter the shape of the distribution. The distribution of capacities is typical for anchors tested in cracked concrete.

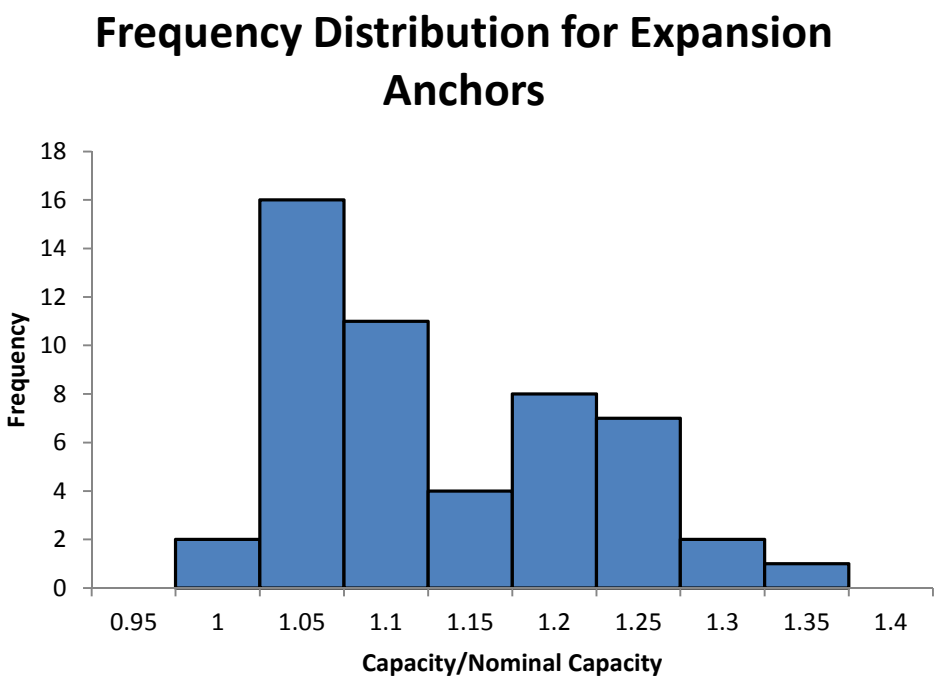

Figure 5-5: Ratios of Tested Capacity to Expected Mean Capacity, Expansion Anchors

The two tests displaying capacities below the expected mean were Anchor A1 in the control specimen and Anchor A2 in the post-installed specimen. Because a ratio of 1.0 represents the expected mean value for breakout tests, it is logical that some values less than 1.0 would occur.

5.4 STATISTICAL VARIATION OF CAPACITIES FOR UNDERCUT ANCHORS

The sample sizes, mean normalized capacities, and coefficients of variation (COV) of capacities are shown in Table 5-4 and Table 5-5, respectively, for each undercut anchor.

Table 5-4: Statistical Distribution of Results for Anchor B1

	n	mean (normalized capacities)	COV (capacities)
Control	6	1.20	0.084
Pre-ASR Installed Anchors/CCI =	6	1.20	0.073
Post-ASR Installed Anchors/ CCI =	5	1.04	0.106

Table 5-5: Statistical Distribution of Results for Anchor B2

	n	mean (normalized capacities)	COV (capacities)
Control	6	0.954	0.021
Pre-ASR Installed Anchors/CCI =	6	1.05	0.016
Post-ASR Installed Anchors/ CCI =	5	0.954	0.019

The normalized mean capacity results for Anchor B1 are greater than 1.0. The COV is smaller than the 15% found in the literature for anchors in cracked concrete. Normalized mean capacities are below 1.0 because steel fracture was the governing failure mode for most tests. The COV found for Anchor B2 tests are lower than for other anchors because the COV for steel failure is smaller than for concrete failure.

Histograms of normalized tensile capacities of Anchors B1 and B2 are shown in Figure 5-6. The histograms are divided by anchor because the failure mode is different for the two embedment depths.

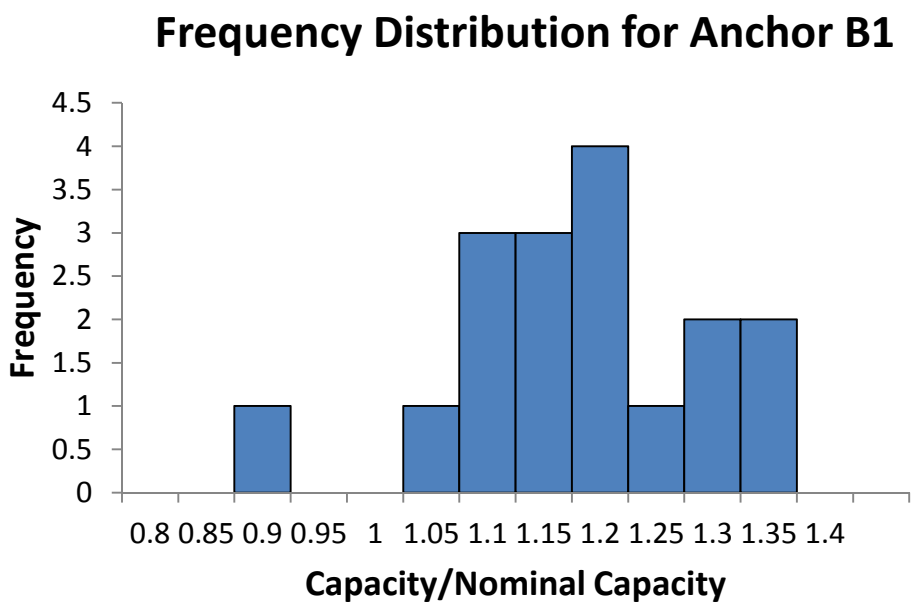

Figure 5-6: Ratios of Tested Capacities to Expected Mean Capacity, Undercut Anchor B1

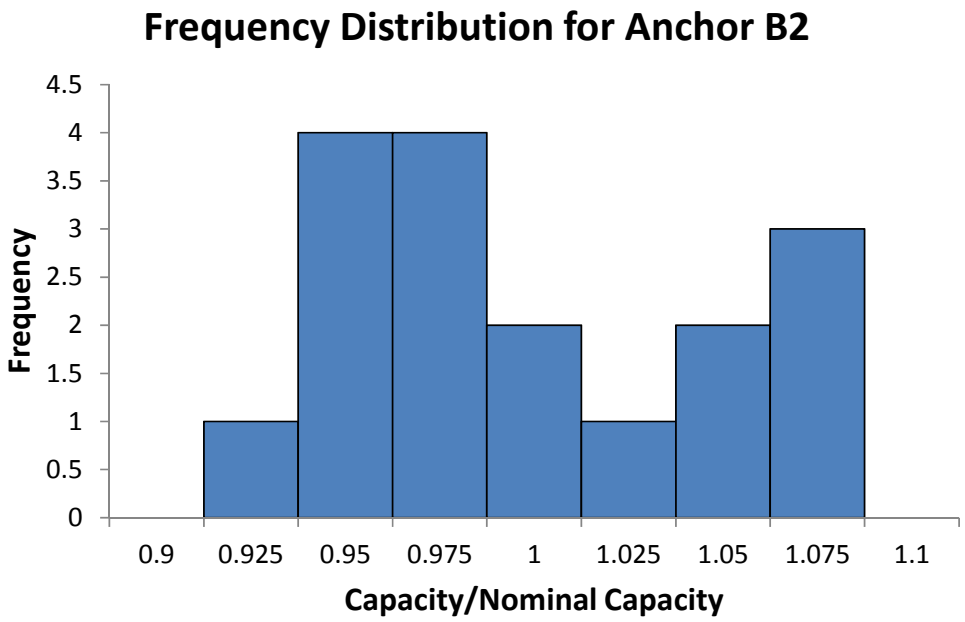

Figure 5-7: Ratios of Tested Capacities to Expected Mean Capacity, Undercut Anchor B2

The histogram for anchor B1 shows normalized tensile capacities above 1.0 with one exception. This test created a breakout cone that included the edge of the specimen. The distribution shows behavior consistent with ACI design.

The histogram for Anchor B2 shows an even spread around a normalized tensile capacity of 1.0. The mean ratios below 1.0 are a result of the embedment depth exceeding critical embedment. Steel fracture is a desirable failure mode.

5.5 EVALUATION OF TEST RESULTS

The results show that tested tensile capacities for both the expansion anchors and undercut anchors do not deviate from expected results in cracked concrete as long as the CCI remains below about 1.5 mm/m. This CCI roughly corresponds to a maximum crack width of 0.15 mm for the specimens used in the anchor testing program.

CHAPTER 6
Summary and Conclusions

6.1 SUMMARY

The investigation described here addresses the tensile capacity and load-deflection behavior of wedge-type expansion anchors and undercut anchors in concrete affected by alkali-silica reaction (ASR). Overall, 85 tensile tests were conducted on control specimens and on ASR-affected specimens. The results of the anchor tests indicate that anchors in concrete cracked due to ASR performed like anchors in concrete cracked due to other mechanisms. Up to a threshold value of the Comprehensive Crack Index (CCI) of at least 1.5 mm/m, all cracking, regardless of cause, has the same effect on the tensile breakout capacity of mechanical and undercut anchors.

6.2 CODE IMPLICATIONS

The design equations of ACI 318 Appendix D and ACI 349 Appendix D, developed for use in cracked concrete, can safely and reliably be used to predict the tensile capacities of anchors in concrete cracked due to ASR, up to CCI values of at least 1.5 mm/m.

6.3 RECOMMENDATIONS FOR FUTURE RESEARCH

The specimens fabricated here used only one concrete mixture and one reinforcement layout. These selections limited the maximum possible expansion of the concrete. Future work could examine the behavior of concrete with more severe ASR degradation, which could increase the threshold CCI above 1.5 mm/m.

Less horizontal and vertical confinement, more transverse confinement

Because of confinement by reinforcement or adjacent structural elements, ASR is not isotropic. Expansion is restrained parallel to reinforcement. Because the specimens here contained no reinforcement oriented perpendicular to the thickness of the affected

members, expansion in that direction was larger than in the other directions. Also, because the CCI recorded cracks found in the horizontal and vertical directions only, transverse expansion was unaccounted for in the quantification of ASR deterioration. To increase the CCI, less reinforcement could be used in the horizontal and vertical directions. For more uniform ASR in all directions, increased reinforcement could be used perpendicular to the free surface. A range of reinforcement ratios would provide insight into the effect of confinement on ASR as it pertains to anchor behavior.

Concrete mixtures of different reactivities

In this test program, for consistency, a single concrete mixture with predicted high reactivity was used for all specimens. If desired, different mixtures with even more reactive constituents could be used to create specimens with even more severe ASR deterioration.

References

ACI Committee 318. (2011). *Building Code Requirements for Reinforced Concrete.* Farmington Hills: American Concrete Institute.

ACI Committee 349. (2006).*Code Requirements for Nuclear Safety-Related Concrete Structures.* Farmington Hills: American Concrete Institute.

ACI Committee 355. (2007). *Qualification of Post-Installed Mechanical Anchors in Concrete.* Farmington Hills: American Concrete Institute.

ACI Committee 355. (2011). *Qualification of Post-Installed Adhesive Anchors in Concrete.* Farmington Hills: American Concrete Institute.

Ahmed, T., Burley, E., Rigden, S., Abu-Tair, A.I. (2003). "The effect of alkali reactivity on the mechanical properties of concrete." *Construction and Building Materials,*17, 123-144.

DeFurio, A., Neuhausen, A., Ramirez, J., Sun, D., Fillip, D., Schell, E., Bacon, J., Bayrak, O., Klingner, R. (2012). "Performance of Post-Installed Anchors in Existing ASR-Affected Concrete." Phil M. Ferguson Structural Engineering Laboratory, The University of Texas at Austin.

Deschenes, D.J. (2009). *ASR/DEF-Damaged Bent Caps: Shear Tests and Field Implications,* MS Thesis, The University of Texas at Austin.

Eligehausen, R. and Fuchs, W. (1987).

Eligehausen, R., and Balogh, T. (1995). "Behavior of Fasteners Loaded in Tension in Cracked Reinforced Concrete." *ACI Structural Journal,* 92(3), 365-379.

Eligehausen, R., and Ozbolt, J. (1992). "Influence of Crack Width on the Concrete Cone Failure Load." 876-881.

Eligehausen, R., Fuchs, W., Lotze, Reuter. (1989).

Eligehausen, R., Mallée, R., Silva, J.F. (2006) *Anchorage in Concrete Construction.* Berlin, Germany: Ernst and Sohn.

Eligehausen, R., Mattis, L., Wollmershauser, R., and Hoehler, M.S. (2004). "Testing Anchors in Cracked Concrete: Guidance for testing laboratories: how to generate cracks." *Concrete International,* 66-71.

Farrow, C.B., Frigui, I., and Klingner, R.E. (1996). "Tensile Capacity of Single Anchors in Concrete: Evaluation of Existing Formulas on an LRFD Basis." *ACI Structural Journal,* 93(1), 128-137.

Folliard, K.J., Barborak, R., Drimalas, T., Du, L., Garber, S., Ideker, J., Ley, T., Williams, S., Juenger, M., Fournier, B., and Thomas, M. (2006). "Preventing ASR/DEF in New Concrete: Final Report." FHWA.

Fournier, B., Bérubé, M., Folliard, K.J., and Thomas, M. (2010). "Report on the Diagnosis, Prognosis, and Mitigation of Alkali-Silica Reaction (ASR) in Transportation Structures" FHWA.

Fournier, B., Ideker, J.H., Folliard, K.J., Thomas, M., Nkinamubanzi, P., and Chevrier, R. (2009). "Effect of environmental conditions on expansion in concrete due to alkali silica reaction (ASR)." *Materials Characterization,* 60, 669-679.

Fuchs, W., Eligehausen, R., and Breen, J.E. (1995). "Concrete Capacity Design (CCD) Approach for Fastening to Concrete." *ACI Structural Journal,* 92(1), 73-94.

Giaccio, G., Zerbino, R., Ponce, J.M., and Batic, O.R. (2008). "Mechanical behavior of concretes damaged by alkali-silica reaction." *Cement and Concrete Research,* 38, 993-1004.

Hallowell, J.M. (1996). *Tensile and Shear Behavior of Anchors in Uncracked and Cracked Concrete under Static and Dynamic Loading,* MS Thesis, The University of Texas at Austin.

Hilti. (2011). *Anchor Fastening Technical Guide,* Hilti, Inc., 5400 South 122nd East Avenue, Tulsa, OK 74146.

ICBO Evaluation Service, Inc. (1992). *Drillco Maxi-bolt Bearing Type, Undercut Anchors.*

Jones, A.E.K., and Clark, L.A. (1996). "The effects of restraint on ASR expansion of reinforced concrete." *Magazine of Concrete Research,* 48(174), 1-13.

Leemann, A., and Merz, C. (2013). "An attempt to validate the ultra-accelerated microbar and the concrete performance test with the degree of AAR-induced damage observed in concrete structures." *Cement and Concrete Research,* 49, 29-37.

Mahrenholtz, C., and Eligehausen, R. (2013). "Dynamic Performance of concrete undercut anchors for Nuclear Power Plants." *Nuclear Engineering and Design,* 265, 1091-1100.

McLeish, A. (1990). "Structural implications of the alkali silica reaction in concrete." Crowthorne: Transportat and Road Research Laboratory, Contractor Report 177.

Nowak, A.S., and Collins, K.R. (2013). *Reliability of Structures.* CRC Press: Boca Raton.

Ostertag, C.P., Yi, C., and Monteiro, P. (2007). "Effect of Confinement on Properties and Characteristics of Alkali-Silica Reaction Gel." *ACI Materials Journal,* 104, 3, 276-282.

Pusill-Wachtsmut, P. (2001) "Performance of Undercut Anchors in Comparison to Cast-in-Place Headed Studs." *International RILEM Symposium on Connections between Steel and Concrete,* 241-250.

Rigden, S.R., Majlesi, Y., and Burley, E. (1995). “Investigation of factors influencing the expansive behavior, compressive strength and modulus of rupture of alkali-silica reactive concrete using laboratory concrete mixes.” *Magazine of Concrete Research*, 47(170), 11-21.

Rivard, P. and Ballivy, G. (2005). “Assessment of the expansion related to alkali-silica reaction by the Damage Rating Index method.” *Construction and Building Materials*, 19, 83-90.

Rodriguez, M. (1995). *Behavior of Anchors in Uncracked Concrete under Static and Dynamic Tensile Loading*, MS Thesis, The University of Texas at Austin.

Shirvani, M. (1998). *Behavior of Tensile Anchors in Concrete: Statistical Analysis and Design Recommendations*, MS Thesis, The University of Texas at Austin.

Smaoui, N., Bissonnete, B., Bérubé, M., Fournier, B., and Durand, B. (2006). “Mechanical Properties of ASR-Affected Concrete Containing Fine or Coarse Reactive Aggregates.” *Journal of ASTM International*, 3(3).

Swamy, R.N., and Al-Asali, M.M. (1988). “Engineering Properties of Concrete Affected by Alkali-Silica Reaction.” *ACI Materials Journal*, 85(5), 367-374.

Vita

Alissa Paige Neuhausen was born in 1988 in Chicago Illinois. She is the first of three children with younger brothers, Jared and Todd. After graduating from Highland Park High School in 2006, Alissa attended the University of California – Berkeley. She obtained a Bachelor of Science in Civil Engineering in 2010. She then enrolled in the Engineering/Public Affairs dual-degree Master's program at the University of Texas at Austin. During her first semester she began working as a research assistant at the Phil M. Ferguson Structural Engineering Laboratory. She received a Master of Science in Engineering and a Master of Public Affairs in August 2014.

Permanent e-mail: alissa.neuhausen@gmail.com

This thesis was typed by the author.